# Nonlinear Behavior of Reinforced Concrete Structures under Seismic Excitation

by

**MATTHEW ANTHONY PIRES**

Bachelor of Science in Civil Engineering
Massachusetts Institute of Technology, 2010



Submitted to the
Department of Civil and Environmental Engineering
In Partial Fulfillment of the Requirements for the Degree of

**MASTER OF ENGINEERING**
**IN CIVIL AND ENVIRONMENTAL ENGINEERING**

at the

MASSACHUSETTS INSTITUTE OF TECHNOLOGY

June 2013



Signature of Author ..........................................................
Department of Civil and Environmental Engineering
May 24, 2013

Certified by ..........................................................
Jerome J. Connor
Professor of Civil and Environmental Engineering
Thesis Supervisor

Accepted by ..........................................................
Heidi Nepf, Chair
Departmental Committee for Graduate Students

# Nonlinear Behavior of Reinforced Concrete Structures under Seismic Excitation

by

MATTHEW ANTHONY PIRES

Submitted to the Department of Civil and Environmental Engineering
on May 24, 2013 in partial fulfillment of the requirements for the
Degree of Master of Engineering in Civil and Environmental Engineering

ABSTRACT

Exploring nonlinear behavior of structures through structural analysis software can be time and computer processing intensive especially with complicated structural models. This paper will explore the nonlinear behavior of a reinforced concrete structure with varying damping conditions that will experience a number of earthquakes at varying intensities. In the effort to produce a more accurate representation of the structural behavior, the building will be designed based on modern design codes. Ultimately, this approach aims to define a range in which engineers can use a linear approximation to determine certain performance metrics like interstory drift and floor accelerations.

Thesis Supervisor: Jerome J. Connor

Title: Professor of Civil and Environmental Engineering

# Acknowledgements

Thank you to Professor Connor and Pierre Ghisbain for being supportive and instructive during the past year and during the development of this thesis.

Thank you to my family and friends for being there for me when I needed you and for being so understanding when the year got busy and I was not able to spend as much time with you.

Thank you to Professor Kocur and the Civil and Environmental Engineering Department for providing me the opportunity to serve as a teaching assistant. Teaching was the highlight of my year. I truly enjoyed my time with the students.

Thank you to the MEng Class of 2013 for making this year special.

# Table of Contents

## List of Figures

# List of Tables

# 1 Introduction

Exploring nonlinear behavior of structures through structural analysis software can be time and computer processing intensive especially with complicated structural models. Finding a way to increase the speed of analyzing large structures with thousands of elements with out losing the accuracy of quantifying the structural and dynamic performance will empower engineers and give them the ability to process more design considerations.

One process to explore is the nonlinear response of reinforced concrete structures during a seismic excitation. This paper will explore the nonlinear behavior of a reinforced concrete structure with varying damping conditions that will experience a number of earthquakes at varying intensities. This research aims to define a range in which engineers can use a linear approximation to determine certain performance metrics like interstory shear deformations and floor accelerations. These metrics can then be used in other analysis to determine lifetime structural costs associated with seismic excitation.

The structure used for analysis was designed according to American Building Code and aims to be an accurate representation of a building frame. The details of this structure have been outline in Chapter 2 of this paper. Providing varying member sizing will create a scenario where individual members will begin to form hinges and experience nonlinear behavior. Other modeling techniques that simplify the design of the structure have groups of structural elements that fail simultaneously and provide an inaccurate representation of building performance and resilience. This sophistication should provide an opportunity for load redistribution and more accurate representation of the load flow after hinge formation.

# 2 Model

In order to explore the linear and nonlinear behavior of a reinforced concrete structure, it was important to develop a model that would be appropriate for conducting multiple earthquake analyses. All models were analyzed using SAP2000 version 15. As an initial simplified approach to this problem, a 2-D model was explored.

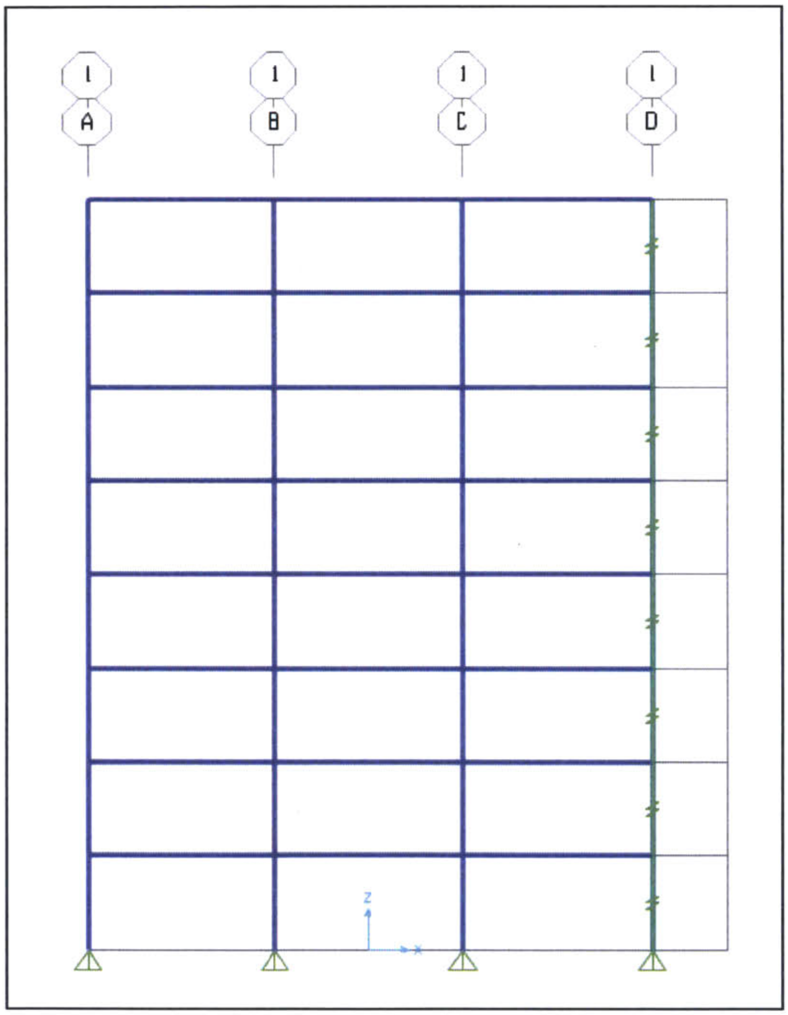


**Figure 1 - 2-D Structure**

The structure is a moment resisting frame that is eight (8) stories tall and each story is 15 feet in height. The building has three (3) bays each spanning 30 feet. Thus, the overall dimensions of the structure are 120 feet in height and 90 feet in width. The aspect ratio is 1.33. With such a relatively small aspect ratio, the building should behave as a shear beam rather than a bending beam. The following sections detail the individual components and properties used to characterize the structure and the technique used to appropriately size the members. An image of the structure is provided in Figure 1.

## 2.1 Material

The structure required the definition of materials - concrete and rebar. The compressive strength of the concrete is 4,000 pounds per square inch and the strength of the rebar is 60,000 pounds per square inch.

## 2.2 Supports

For the purpose of the analysis, geotechnical conditions were not considered and all earthquake loading was applied at the base of the structure. Support conditions were assumed to be fixed though it is understood that these conditions are difficult to deploy in the field.

## 2.3 Loading

The structure was designed for realistic dead and live loads for an office building located in a high- wind coastal region. The structure is a 2-D representation of a structure with 6 inch slabs. The gravity and lateral loads considered are noted in Table 1. These loads were used to define the static load patterns, which eventually were used to define the section properties.

**Table 1 - Loads**

| Loads | Loading (psf) |
| --- | --- |
| Dead (Slabs) | 75 |
| Superimposed Dead Load | 20 |
| Live Load (Office Building) | 100 |

It is important to note that the live load was separated into three (3) conditions, each representing the distributed loading on each structural bay. These patterns were assembled according to the load combinations guidelines of ASCE 7 – Minimum Design Loads of Buildings and Other Buildings. Though wind load is commonly considered in design for a structure of this height, the live load combinations governed the design. Figure 2 shows the load combinations applied to the structure. These load combinations were amalgamated into an envelope condition and ultimately used to determine the governing stress in the beams and columns. The beams were governed by the maximum moment and though the columns experience some moment, the axial load governed the design.

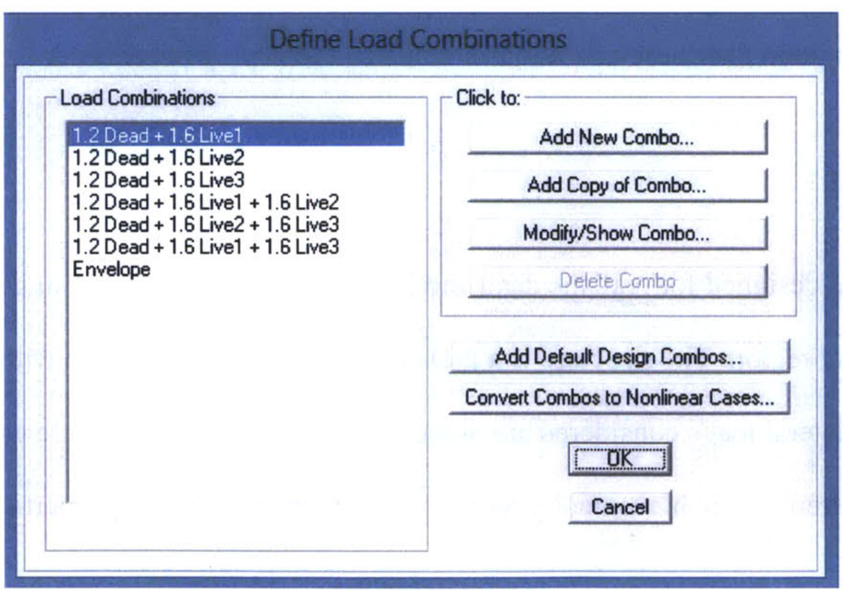


**Figure 2 - Load Combination Menu**

## 2.4 Beam and Column Design

With the geometry, support conditions and loading, the structure was generated within the software. Once these design criteria were established, the beams and columns could be designed. For the beam, initial dimensions were selected and the concrete cover for the rebar was assumed to be 2.5 inches. The maximum moment, $M_u$, and the effective depth of the beam can be used to determine the area of steel required.

$$J_d = 0.875 * d - C_c$$

where,

$J_d$, effective depth of the beam

$d$, nominal depth of the beam

$C_c$, concrete cover

The area of the steel can be determined with the equation below, which is applicable for load resistant factored design (LRFD).

$$a_{st} = \frac{M_u}{\phi * f_y * J_d}$$

where,

$a_{st}$, area of steel

$M_u$, factored moment (LRFD)

$f_y$, yield strength of rebar

$J_d$, effective depth of the beam

$\phi$, load resistance factor, 0.9 for LRFD

This value should be compared to the minimum steel requirement within ACI318. Once the amount of steel is calculated, a practical number of rebar needed in the beam can be determined. This amount of steel can then be used to determine the capacity of the beam. The height of the compression block needs to be calculated first using the equation below.

$$a = \frac{A_{st} b_w}{0.85 f_c' f_y}$$

where,

a, height of the compression block

$A_{st}$, total area of non-prestressed longitudinal reinforcement

$b_w$, beam width

$f'_c$, specified compressive strength of concrete

$f_y$, specified yield strength of reinforcement

The moment capacity of the beam can be defined using the height of the compression block. The equation below illustrates this relationship.

$$M_n = A_{st} f_y (h - C_c - \frac{a}{2})$$

$$M_u = \phi M_n$$

where,

$M_n$, nominal moment capacity of the beam

$A_{st}$, total area of non-prestressed longitudinal reinforcement

$f_y$, specified yield strength of reinforcement

h, nominal height of the beam

$C_c$, concrete cover

a, height of the compression block

$M_u$, ultimate moment capacity of the beam

$\phi$, load resistance factor, 0.9 for LRFD

The ultimate moment capacity of the beam must exceed the maximum moment experienced by the beam; otherwise the dimensions of the beam should be modified until this requirement is met.

The columns were designed for the maximum axial load since the maximum moment is small in comparison. The maximum axial load will define the maximum nominal load.

$$\phi P_n = P_u$$

where,

$P_n$, nominal axial load

$P_u$, ultimate axial load

$\phi$, load resistance factor, 0.9 for LRFD

To define the required size of the column, an area of steel to area of gross area ratio should be prescribed. Using this ratio an estimation of the gross area can be established. The gross area can be calculated using the Equation 10-1 from Section 10.3.6.1 in ACI 318. In the case, the assumption is that the spiral reinforcement conforms to Section 7.10.4 of ACI 318

$$\phi P_{n,max} = 0.85\phi[0.85 f_c'(A_g - A_{st}) + f_y A_{st}]$$

where,

$P_{n,max}$, maximum allowable nominal axial strength of cross section

$f'_c$, specified compressive strength of concrete

$A_g$, gross area of concrete section

$A_{st}$, total area of nonprestressed longitudinal reinforcement

$f_y$,  specified yield strength of reinforcement

If the right side of the equation is multiplied by the unity of $A_g$, the resulting equation takes the following form:

$$\phi P_{n,max} = A_g 0.85\phi[0.85f_c'\left(\frac{A_g}{A_g} - \frac{A_{st}}{A_g}\right) + f_y\frac{A_{st}}{A_g}]$$

The equation can now be simplified and the variables can be rearranged in order to solve for $A_g$.

$$A_g = \frac{\phi P_{n,max}}{0.85\phi[0.85f_c'\left(1 - \frac{A_{st}}{A_g}\right) + f_y\frac{A_{st}}{A_g}]}$$

In this equation, $A_{st}$ / $A_g$ is a prescribed ratio. The gross area governs the dimensions of the column. The area of steel to gross area ratio will define the area of the steel needed in the column. As in the beam design, a practical number of rebar whose area exceeds the area determined from the previous calculation should be determined. In the design of the structure for this analysis, the columns were designed in groups characterized by location.

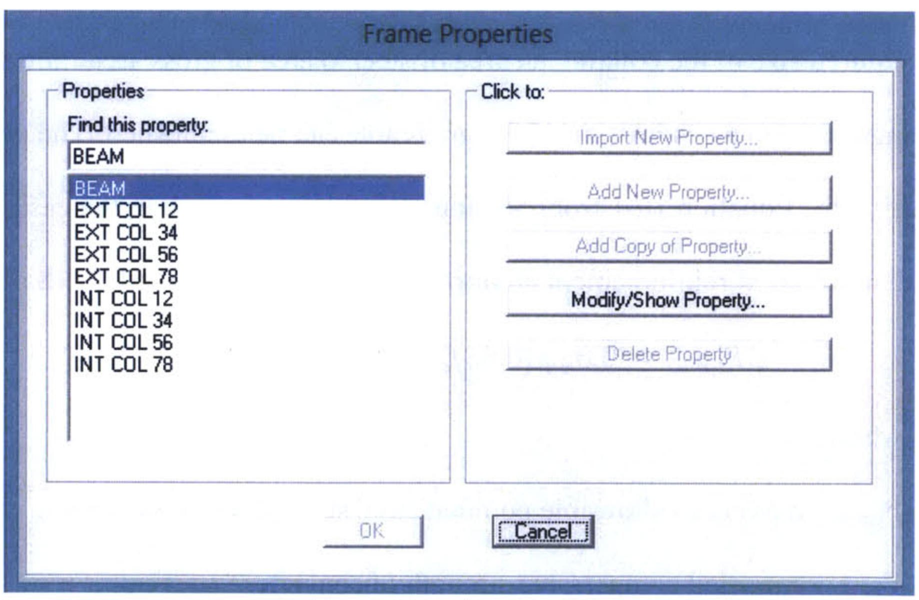


**Figure 3 - Frame Properties**

The interior columns were designed as a separate column compared to the exterior columns. The columns were grouped every two floors to mimic the practical design of columns for buildings. It is typical that the column dimensions would be consistent for several stories at a time. The beam and column designs were defined as frame section and can be seen in the Figure 3. Each section property is governed by the loading and can be represented using the section creator. Figure 4 shows the section created for the beam elements. The only parameters changed were the depth and the width of the beam.

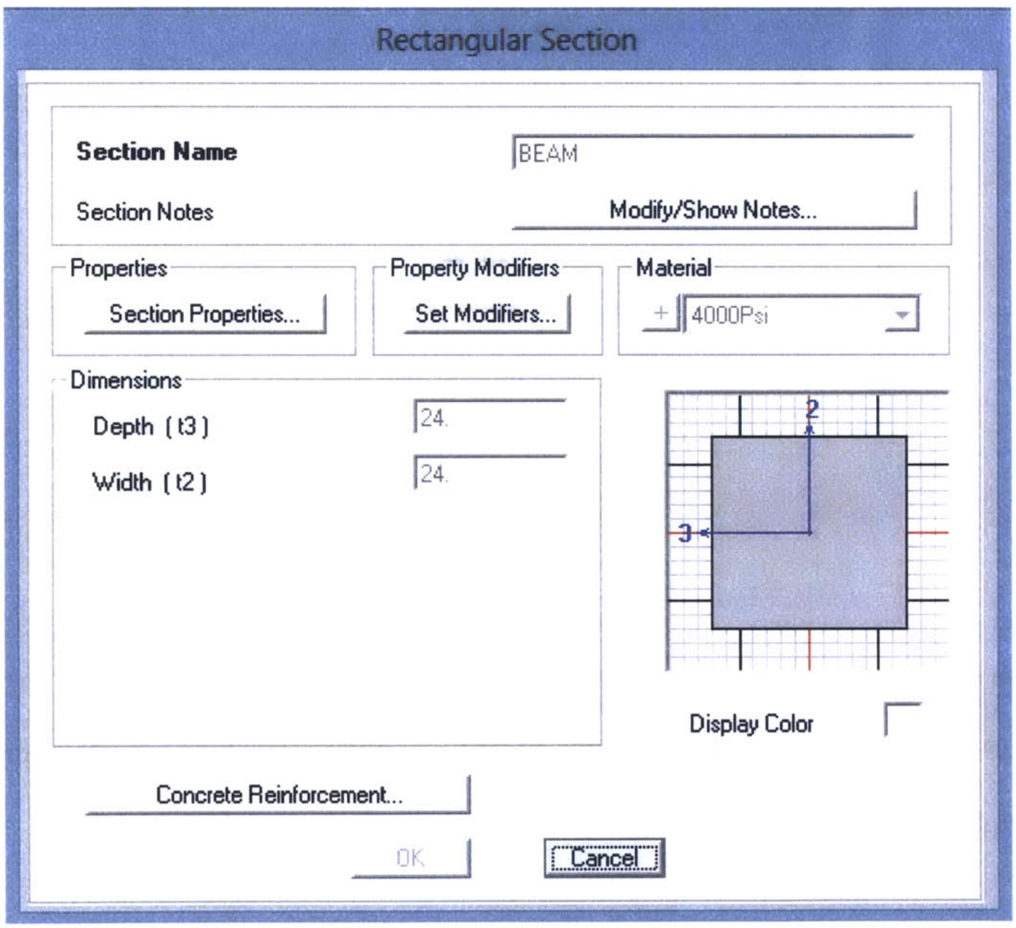


**Figure 4 - Beam Section**

The reinforcement data calculated in the previous section can be inputted using the "Concrete Reinforcement" menu. Longitudinal and Confinement Bars were assumed to be A615 Grade 60

Steel and the concrete cover was 2.5 inches. Figure 5 shows the reinforcement menu for beam elements.

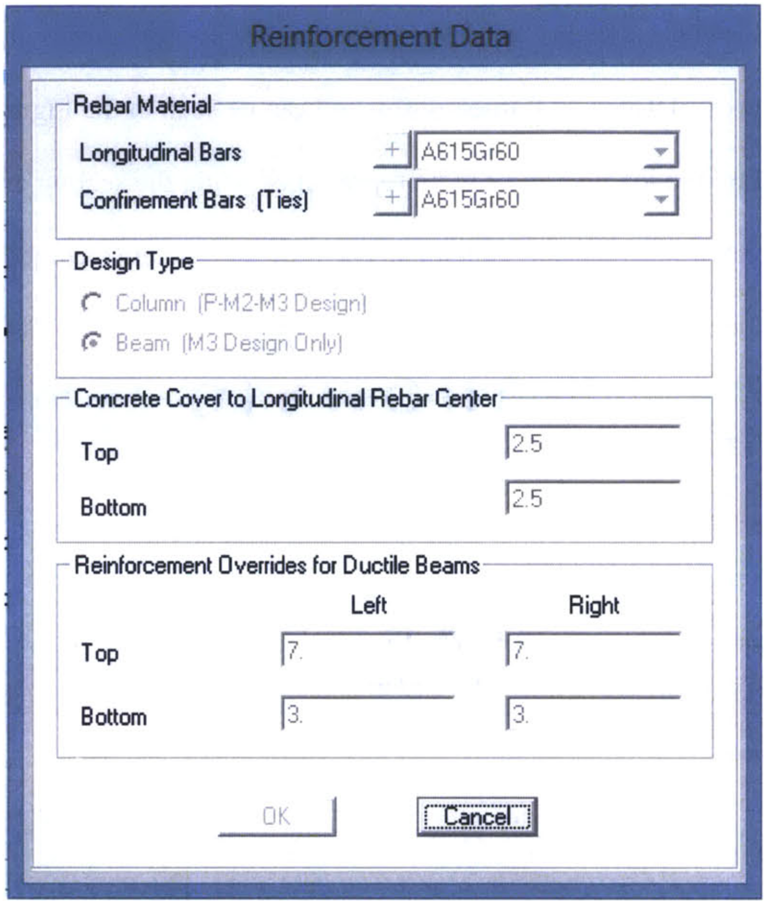


**Figure 5 - Reinforcement Data - Beam**

The column sections were generated in a similar fashion. The only default parameter that needed to be altered in the section properties was the dimensions of the column. The reinforcement menu, though, required slightly different information to properly model the element.

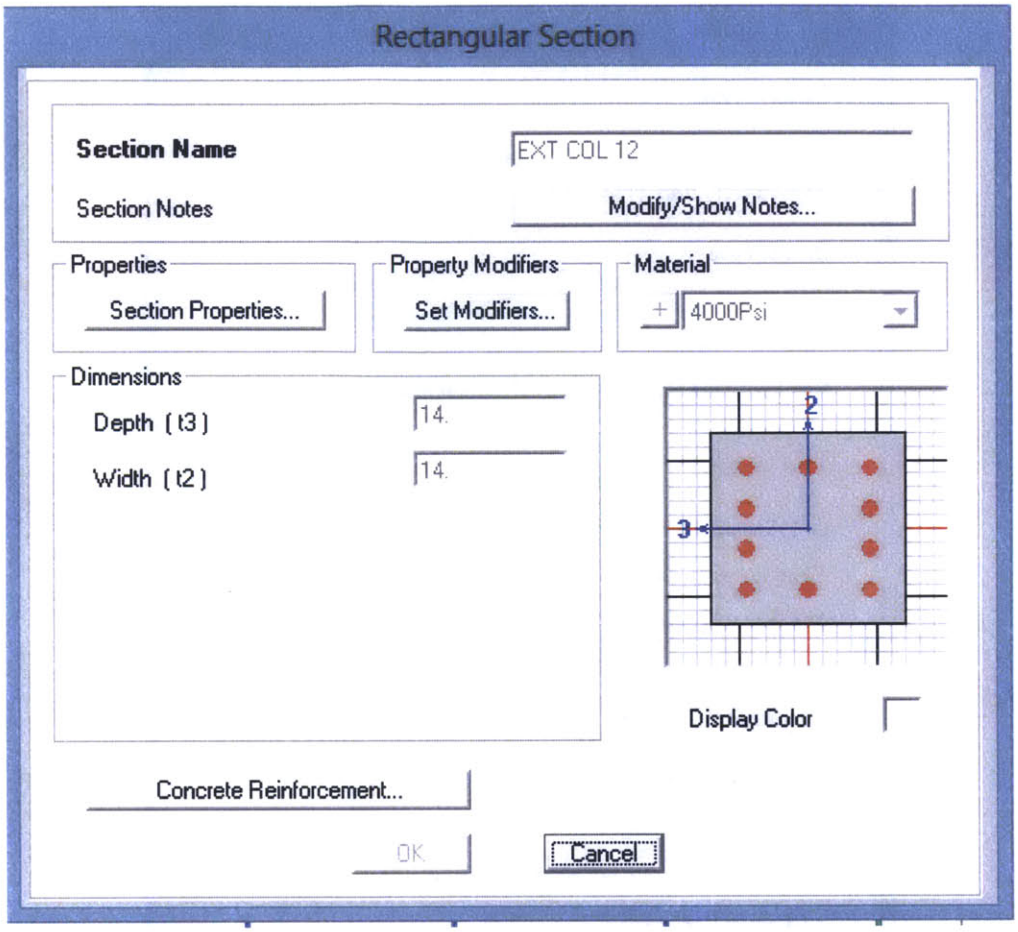


**Figure 6 - Column Section**

The column reinforcement used the same longitudinal and confinement bars as the beams. The concrete cover for the columns were considered to be 1.5 inches The number of longitudinal bars on the 2-dir or 3-dir face depended on the number of bars necessary to develop the full capacity of the column. The 2-dir and 3-dir faces are the local axes of the column and are visible in the cross-section image in Figure 6. The orientation of the bars can be seen in the Figure 6. This can be an iterative process. It is vital that the bars fit appropriately within the cross-sectional area. In order to solve crowding or sparse area issues, the bar quality should be adjusted and different size rebar should be considered. The confinement bars were always considered to be #4 bars at 6 inch spacing.

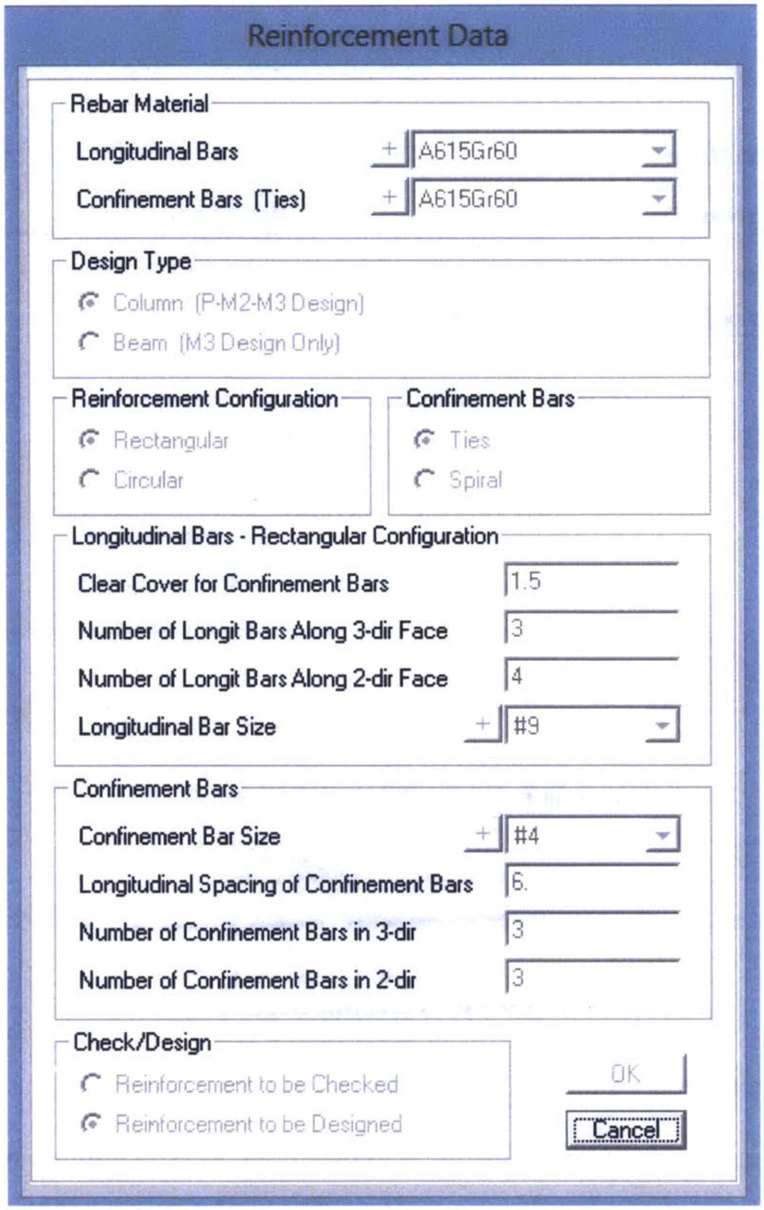


**Figure 7 - Reinforcement Data - Column**

The beam and column sizes determined through these can be found in the Appendix. A modal analysis was conducted with these sections to determine the mode shapes and periods. These values were important when defining the load cases for the time history analysis. The periods of the structure are shown in Table 2.

**Table 2 - Modal Information**

| Mode | Period (sec) | Frequency (Hz) | Modal Participation Factor |
|---|---|---|---|
| 1 | 1.66 | 0.60 | 0.8566 |
| 2 | 0.70 | 1.44 | 0.9627 |
| 3 | 0.40 | 2.48 | 0.9885 |

The modal information can provide some insight into the damping ration of each mode based on the modal frequency and damping ratios used. The modes shapes of the structure can be seen in Figure 8.

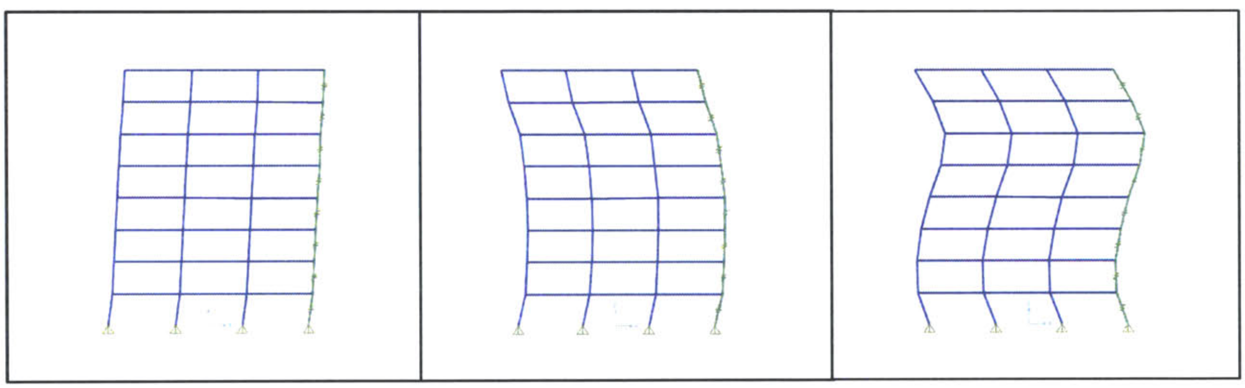

**Figure 8 - First three (3) mode shapes of the structure**

Rayleigh equation can be very useful in this situation to determine the governing mode shape. The Rayleigh damping parameter can be defined in terms of the mass and stiffness of the structure.

$$c = 2\omega_i\xi_i = \alpha m + \beta k$$

where,

c Rayleigh damping parameter

$\alpha$ mass damping parameter

| | |
|---|---|
| m | mass of the structure |
| β | stiffness damping parameter |
| k | stiffness of the structure |
| $\omega_i$ | frequency of mode i, also defined as the square root of $k_i/m_i$ |
| $\xi_i$ | damping ratio of mode i |

The mass and stiffness damping parameters can be defined from the equations below.

$$\alpha = \frac{2\omega_i\omega_j}{\omega_j - \omega_i}(\omega_j\xi_i - \omega_i\xi_j)$$

$$\beta = \frac{2}{\omega_j^2 - \omega_i^2}(\omega_j\xi_j - \omega_i\xi_j)$$

Now taking the frequencies from the first and second mode and considering 5% for the structure, will generate the following values of α and β.

$$\alpha = \frac{2(0.60)(1.44)}{1.44 - 0.60}[(1.44)(0.05) - (0.60)(0.05)] = 0.086$$

$$\beta = \frac{2}{(1.44)^2 - (0.60)^2}[(1.44)(0.05) - (0.60)(0.05)] = 0.049$$

The initial equation can be written and the values of α and β can be assigned.

$$\xi_i = \frac{0.086}{2\omega_i} + \frac{0.049\omega_i}{2}$$

The Rayleigh damping ratios associated with the first three modes can be calculated with this equation and generates a damping ratio of 8.6% for the first mode, 6.5% for the second mode, and 7.8% for third mode. This indicates that second mode will experience the least amount of damping and will have the greatest effect on the performance of the structure.

## 2.5 Hinges

Each beam and column element requires hinge elements to properly analyze the nonlinear behavior of the structure. The hinge elements were assigned to either end of the column and beam elements. The menu can be seen in Figure 9. As the intensity of the earthquakes increases, the moment experienced within the beams and columns also increases. At some point, the moment experienced by these elements will exceed the capacity and a hinge will form, the load will shift, and the system will release energy due to the hysteretic moment rotation behavior assumed for plastic hinges.

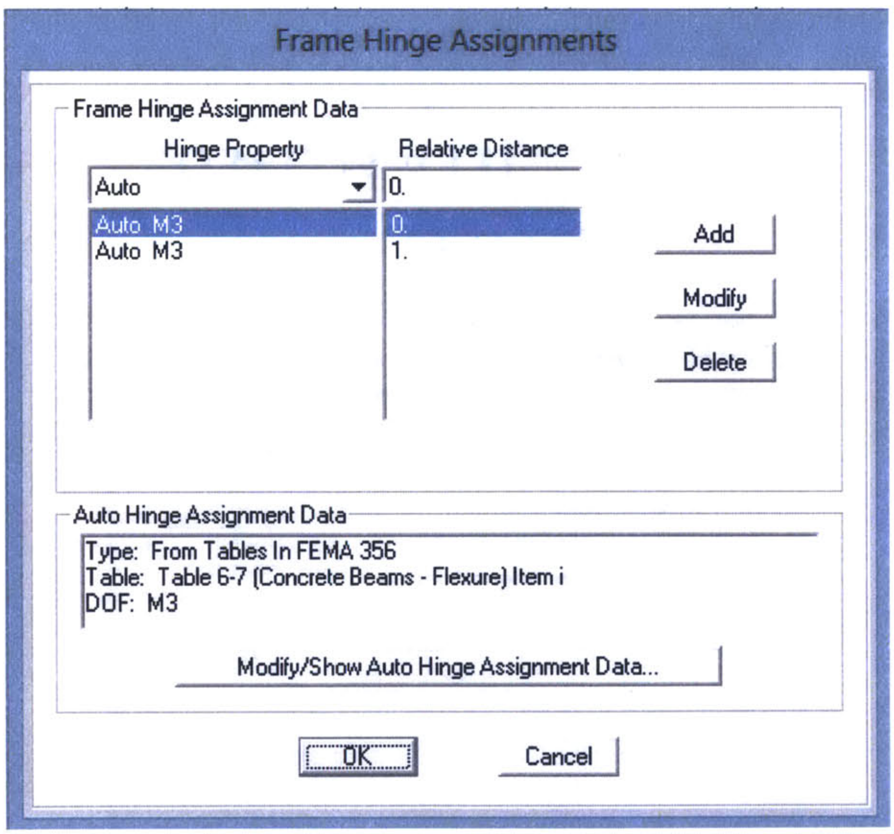


**Figure 9 - Frame Hinge Assignments**

# 3 Analysis

## 3.1 Link

It is important to record the drift of each floor after the analysis cases run. Links that have no weight or stiffness were introduced along one face of the structure. The link deformation values can be easily exported using the SAP output tables. The links span from floor-to-floor so the percent drift for each story will be the local deformation of the link divided by the length of the link (or story). The details that describe the link are shown in Figure 10. The link will be linear and thus will measure the deformation in only one direction and not the resultant of several directional deformations.

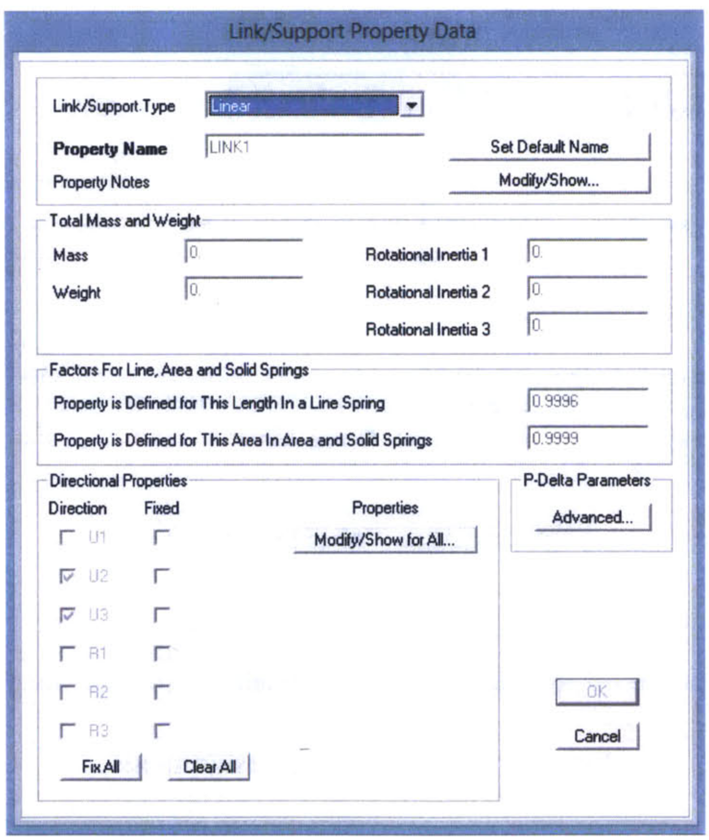


**Figure 10 - Link/Support Property Data**

## 3.2 Time History Definition

The time history information was adopted from earthquake data acquired from the Pacific Earthquake Engineering Research Center Database. The frequency spectrum is normalized in terms of g and can be scaled to match any intensity desired. The earthquake information is provided in Table 3.

**Table 3 - Earthquake Data**

| No. | Earthquake | Station | Time Step |
|---|---|---|---|
| 068 | SAN FERNANDO 02/09/71 14:00 | LA HOLLYWOOD STOR LOT | 0.01 |
| 985 | LOMA PRIETA 10/18/89 00:05 | ANDERSON DAM DOWNSTREAM | 0.005 |
| 995 | LOMA PRIETA 10/18/89 00:05 | COYOTE LAKE DAM DOWNST | 0.005 |

The information for each earthquake provides spectrum similar to that seen in the **Error! Reference source not found.**.

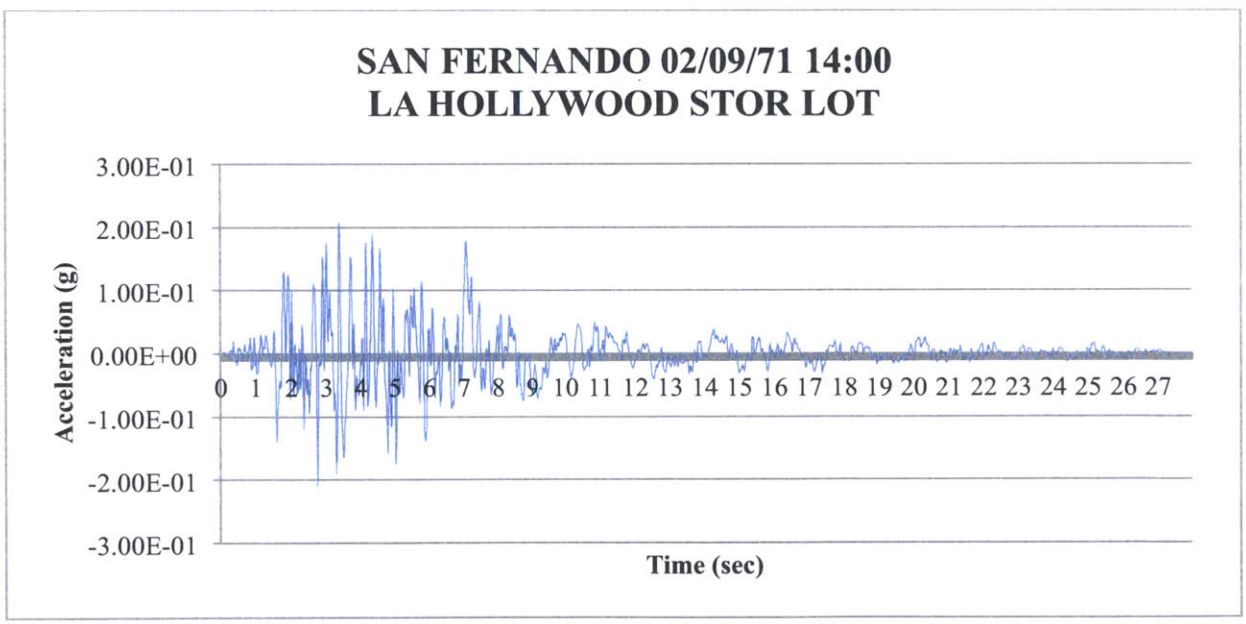


**Figure 11 - San Fernando Earthquake at Hollywood**

For each earthquake, intensities between 0.1g and 1.0g were considered. This information can be defined within the SAP's Time History Function Definition menu. An image of this menu is shown in Figure 12.

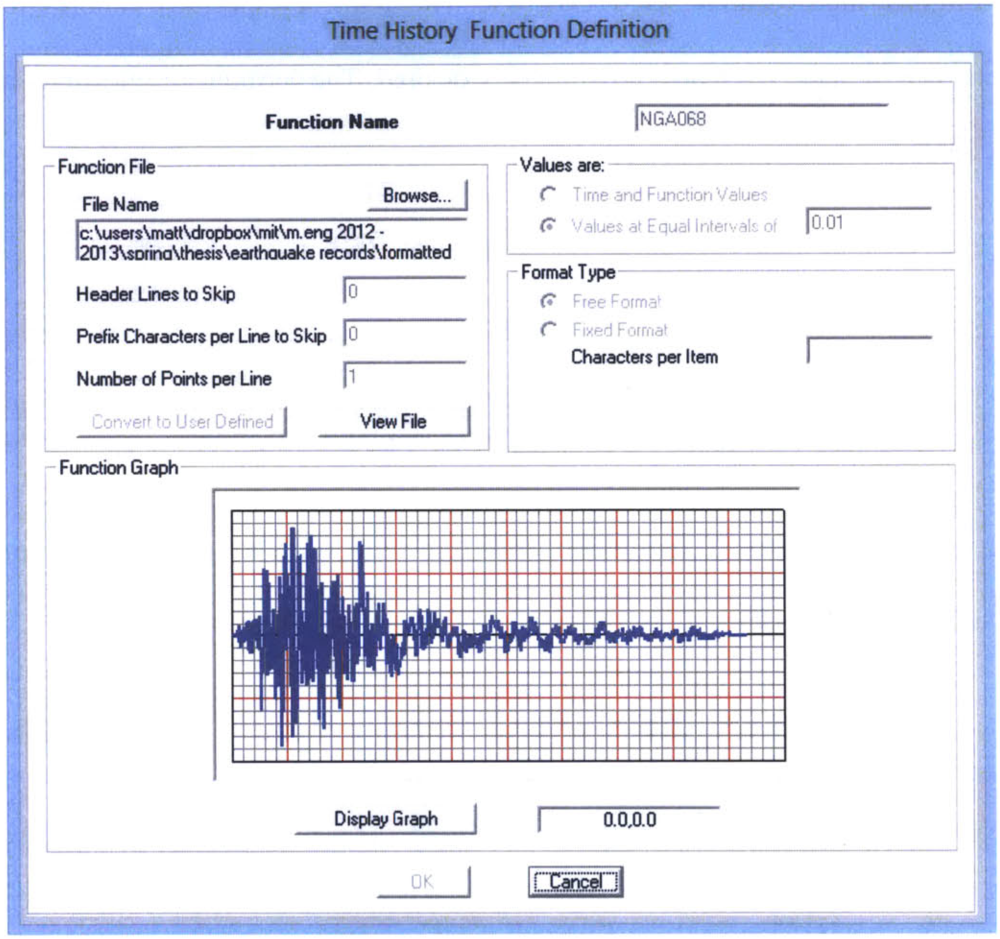


**Figure 12 - Time History Function Definition**

## 3.3 Time History Load Cases

Once the time histories are properly defined within the SAP software, the load cases can be generated. In the load case menu, picture below, certain selections were made. Under the load case type drop time, a "Time History" approach should be selected. This will alter the "Loads Applied" section. The "Analysis Type" and "Time History Type" were nonlinear and direct integration respectively. The "Initial Condition" of the system was an unstressed state. Under the "Loads Applied" section the "Accel" type was selected for load in the local U1 direction. Depending on the earthquake, the function would change to match the appropriate function. The scale factor was used to meet the correct intensity needed. As previously mentioned, all earthquakes were normalized in terms of g. The maximum frequency within the earthquake data was scaled to meet the intensity requirement. The factors also need to match the units used throughout the model.

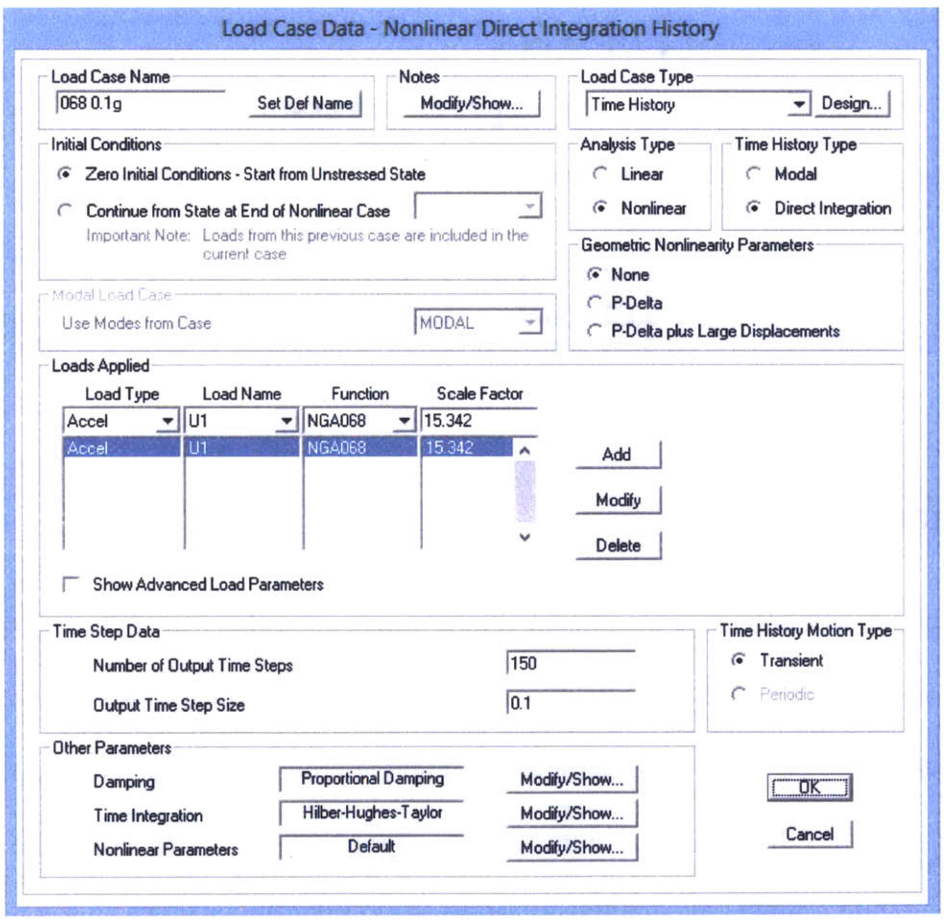


**Figure 13 - Load Data – Nonlinear Direct Integration History**

Within the "Damping" menu, the damping coefficient was defined by the period of the structure. The periods of the first and second mode, as defined by the modal analysis, were used with 5%

damping, which is a conservative estimate for concrete structures and allowed by building code. These values will automatically generate the "Mass Proportional Coefficient" and "Stiffness Proportional Coefficient" necessary for the nonlinear analysis.

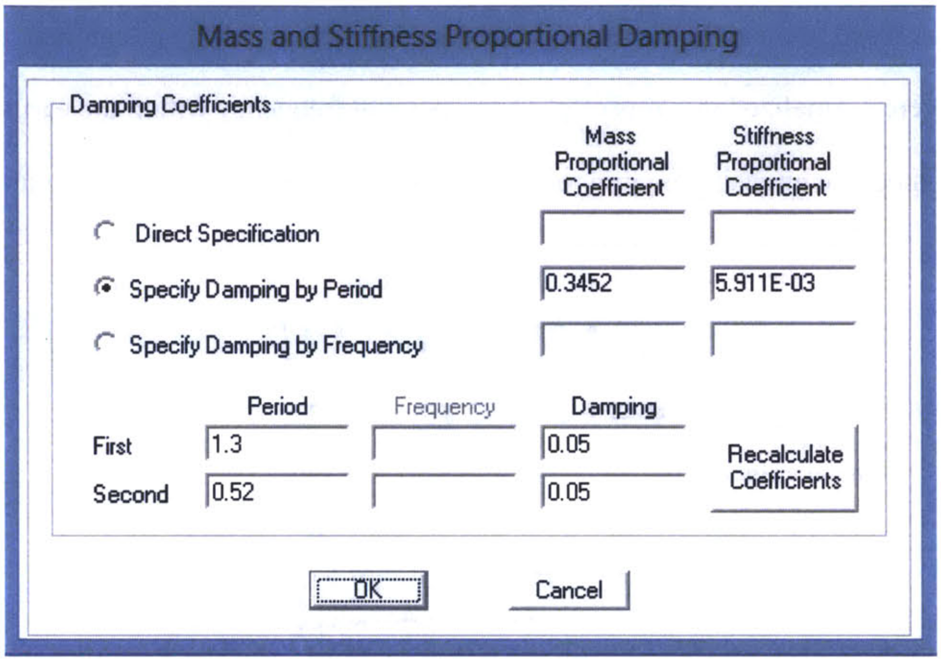


**Figure 14 - Mass and Stiffness Proportional Damping**

## 3.4 Dynamic Approach

Based on a number of earthquake time histories, the building was hit with a number of intensities. For each intensity, a value of the maximum lateral deformation was record in each link. These values can be normalized to the story height to produce the interstory drift ratio. These values could then be compared to the linear analysis to determine where in the analysis the linear can accurately estimate the nonlinear performance of the structure. The acceleration for each floor was approached in a similar manner. These accelerations can be compared to the values for the linear case to determine where in the analysis the linear case can accurately estimate the acceleration of the nonlinear approach.

# 4 Results

Once the SAP2000 analysis has run, the output tables can be interpreted to provide further insight in the deformation of the links and acceleration of each story. The shear deformation of each link is normalized to the story height and can be plotted as shown in Figure 15. This figure shows the shear deformations observed on the nonlinear analysis for each link over a range of intensities.

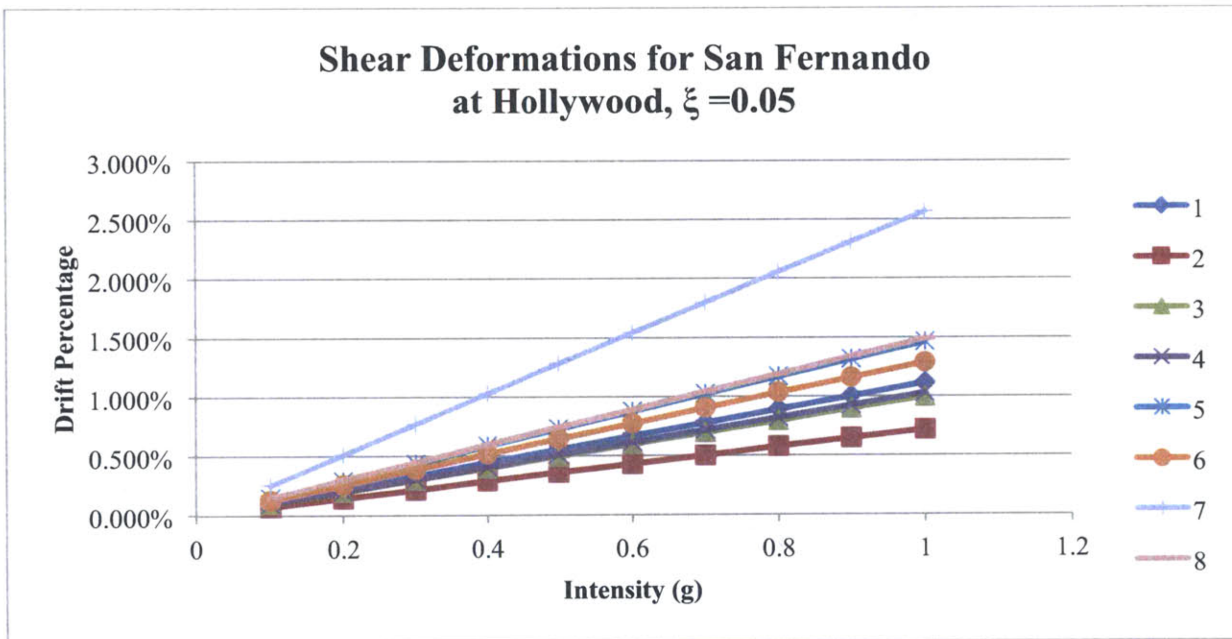


**Figure 15 - Nonlinear Shear Deformation for San Fernando at Hollywood, $\xi$ =0.05**

The same procedure can be performed with a linear analysis of the structure. The linear analysis was run with one (1) intensity and then these results were scaled for the remaining intensities. The linear shear deformations can be seen in Figure 16. The nonlinear and linear deformations are identical. The shear deformation plots for the remaining two (2) earthquakes can be found in the Appendix. These analyses garnered the same results. The linear and nonlinear deformations were identical.

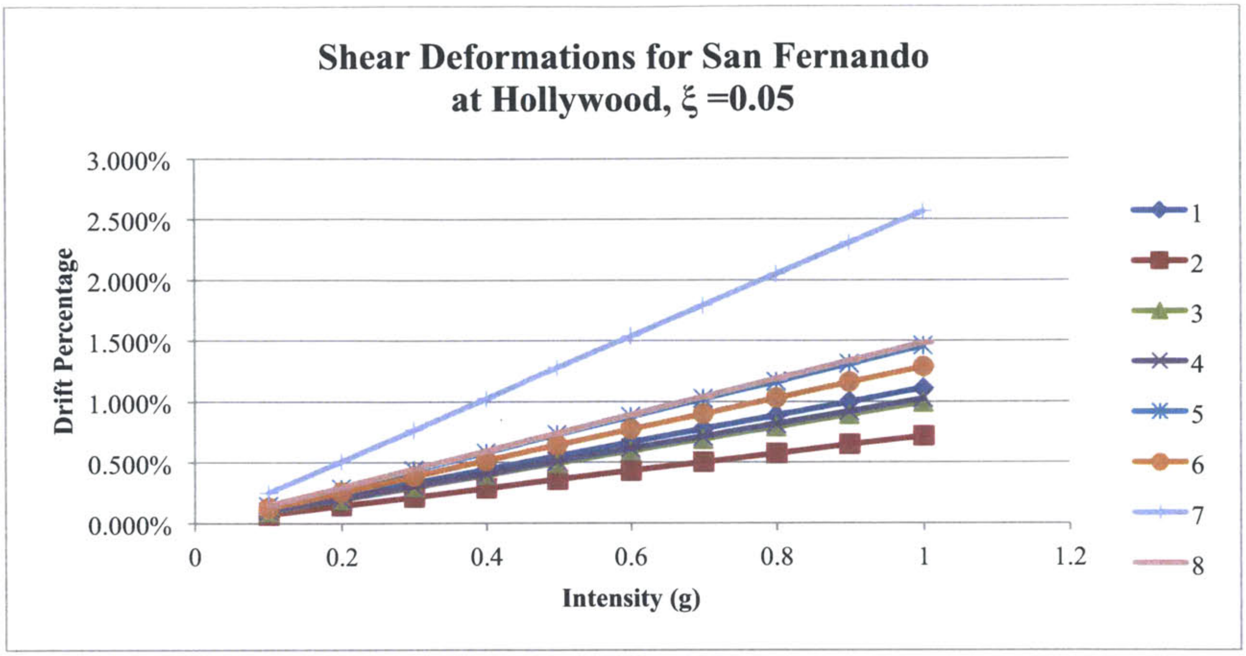


**Figure 16 - Linear Shear Deformations for San Fernando at Hollywood, $\xi$ =0.05**

The acceleration of each story can also be scaled using the 0.1g behaviors in order to compare the linear and nonlinear behavior. Figure 17 below shows the nonlinear accelerations due to the San Fernando earthquake.

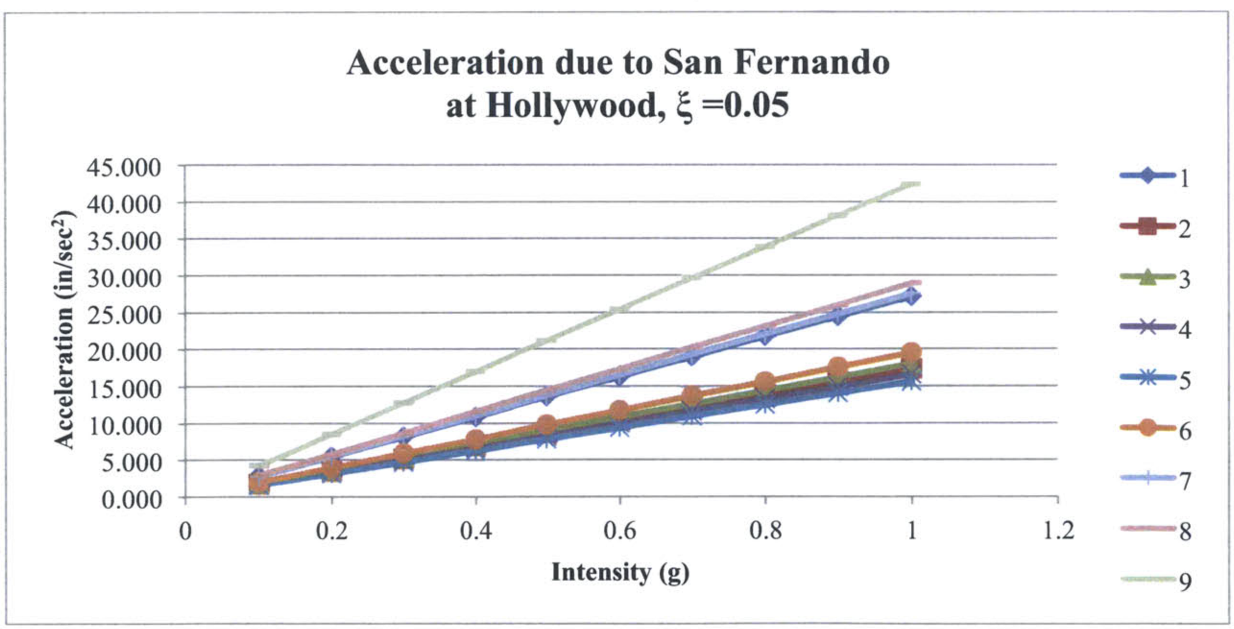


**Figure 17 - Nonlinear Accelerations for San Fernando at Hollywood, $\xi$ =0.05**

The nonlinear accelerations match the linear results shown in Figure 18.

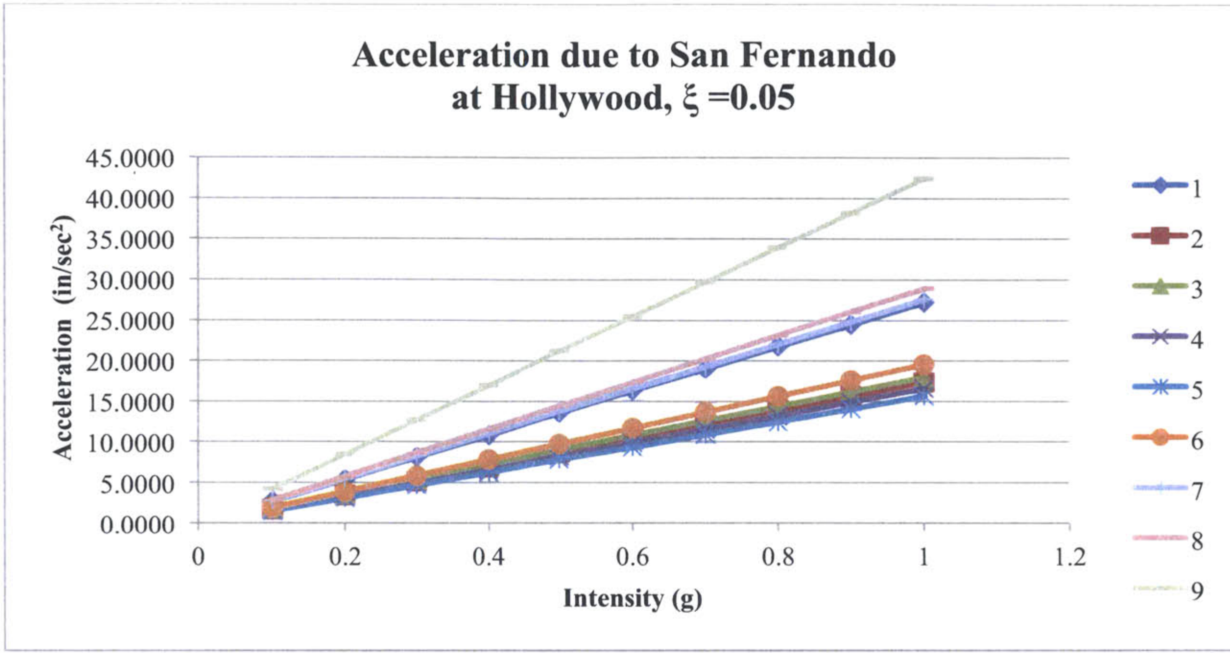


**Figure 18 - Linear Acceleration for San Fernando at Hollywood, $\xi$ =0.05**

These results were unexpected. The hypothesis was that the structure would begin to experience nonlinear behavior before 1.0g, since this is considered a significant earthquake. The results show that based on these approximations and this 2-D representation that the interstory drift deformation and the floor accelerations can be approximated using a linear approach instead of a nonlinear approach.

These results sparked research into the behavior of the structure. There was some motivation to explore the intensity at which the structure would begin to experience nonlinear deformation. The intensity of the San Fernando earthquake was increased until nonlinear deformation was noticed. Figure 19 shows the behavior of the links between 0 and 5g. For clarity, only odd valued intensities are depicted in the graph. The nonlinear behavior begins at 3.2g and happens primarily in link 7. Recall that the column size transitioned from link 6 to 7. Though sized appropriately, the columns on this floor developed hinges creating a mechanism and creating the nonlinear deformation in the link. The deformation in link 8 remained linear in this range.

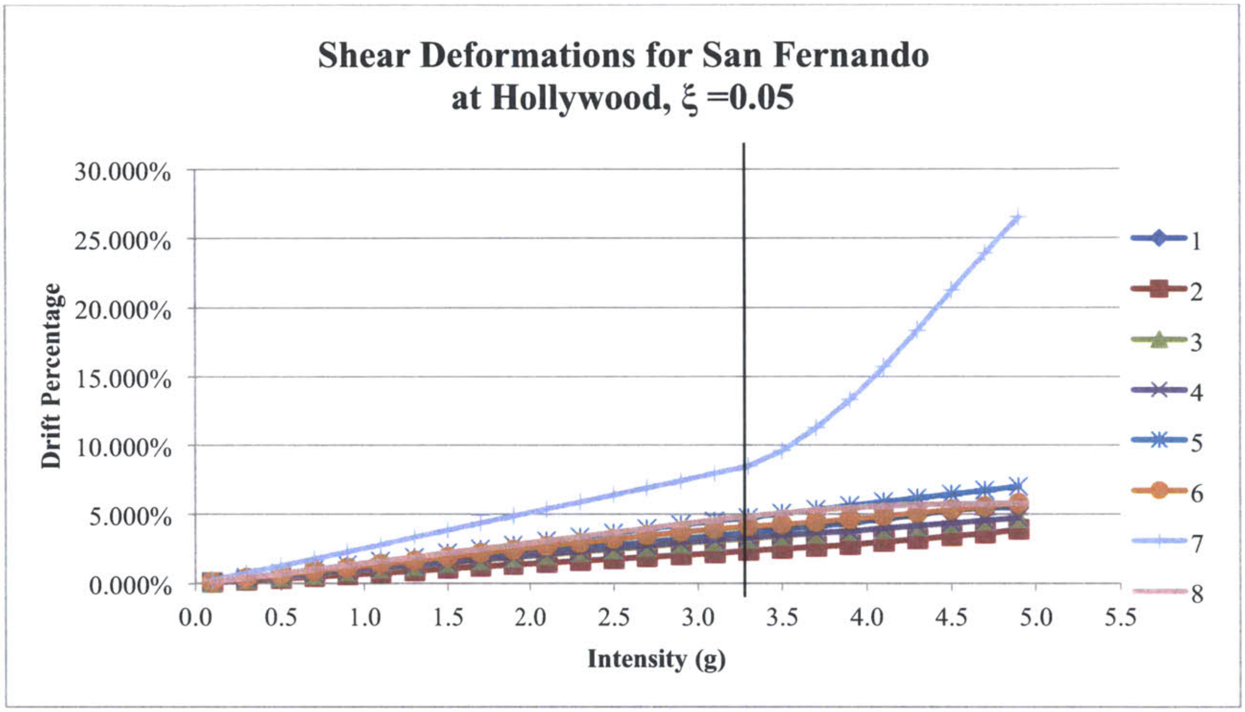


**Figure 19 - Nonlinear Shear Deformation until nonlinear response for San Fernando, $\xi$ =0.05**

Knowing that the nonlinearity occurs in this range, the nodal accelerations can also be analyzed. Figure 20 shows the nonlinear behavior of the accelerations also occured at 3.2g. Only the odd valued intensities have been shown for clarity. The three (3) top nodes of these structure that coincide with the 7$^{th}$ floor, 8$^{th}$ floor and roofline experienced the nonlinearity and ultimately lead to the formation of hinges at the 7$^{th}$ floor.

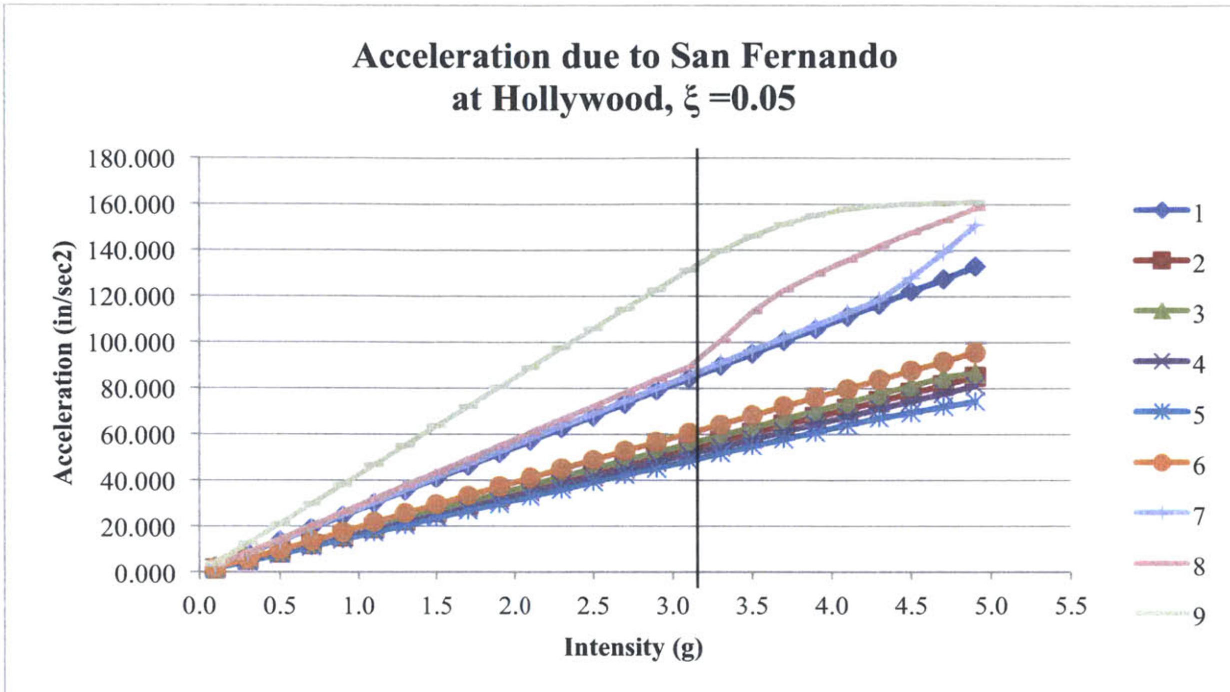


**Figure 20 - Nonlinear Accelerations until nonlinear response for San Fernando, $\xi$ =0.05**

As mentioned prior, the typical damping ratio of reinforced concrete structures was 5%. In some cases, the reinforced concrete structures might have less damping and in order to quantify the linear and nonlinear effects two (2) additional damping ratios were considered, 1% and 3%.

Figure 21 shows the nonlinear shear deformations due to the San Fernando earthquake with the structure having 3% damping. The intensity was increased until nonlinear behavior occurred. The structure experienced nonlinear behavior at the same intensity as the initial structure with 5% damping. As in the initial model, the 7$^{th}$ link is the first section to experience this behavior.

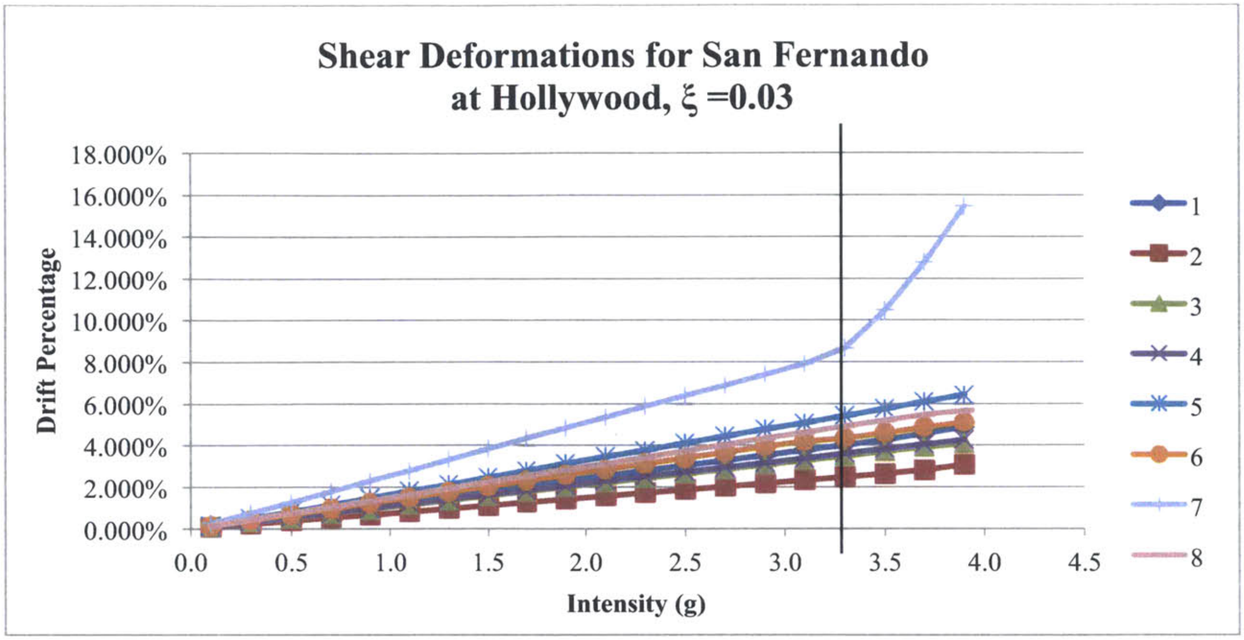


**Figure 21 - Nonlinear Shear Deformations for San Fernando at Hollywood, ξ =0.03**

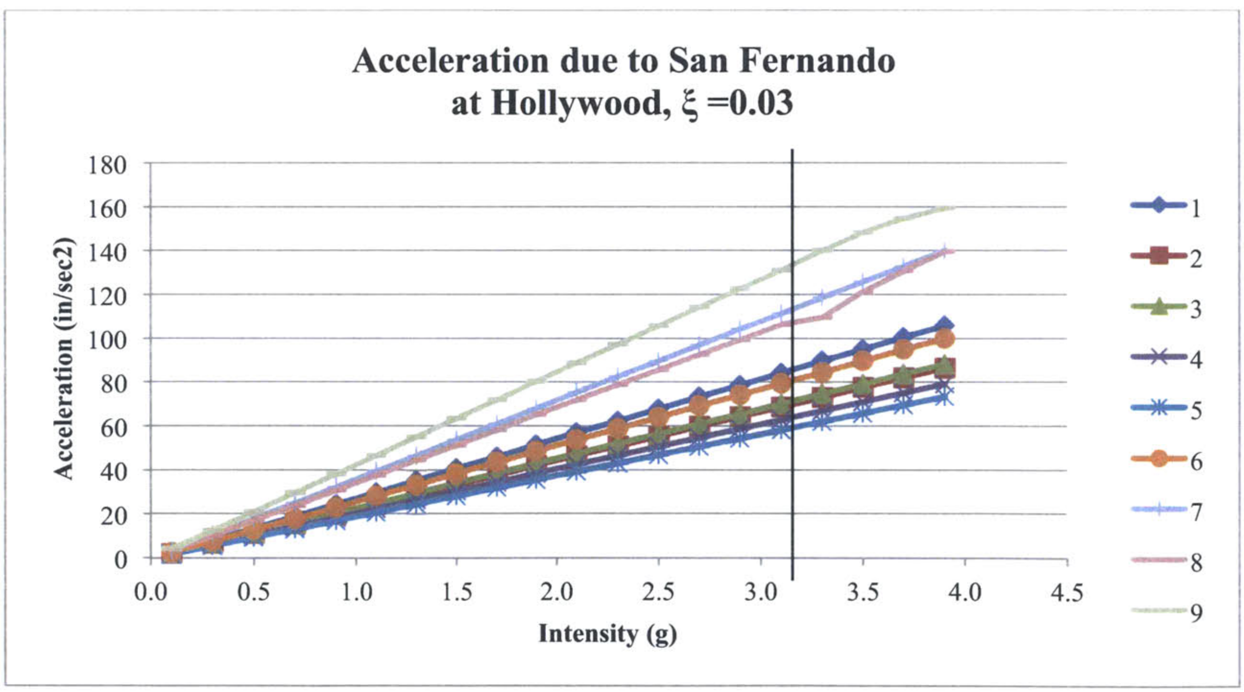


**Figure 22 – Nonlinear Accelerations for San Fernando at Hollywood, ξ =0.03**

The acceleration shown in Figure 22 also experiences nonlinear behavior in the 3.3g intensity region. Despite this significant decrease in the damping ratio, the structure continues to behave linearly within below the 1.0g range.

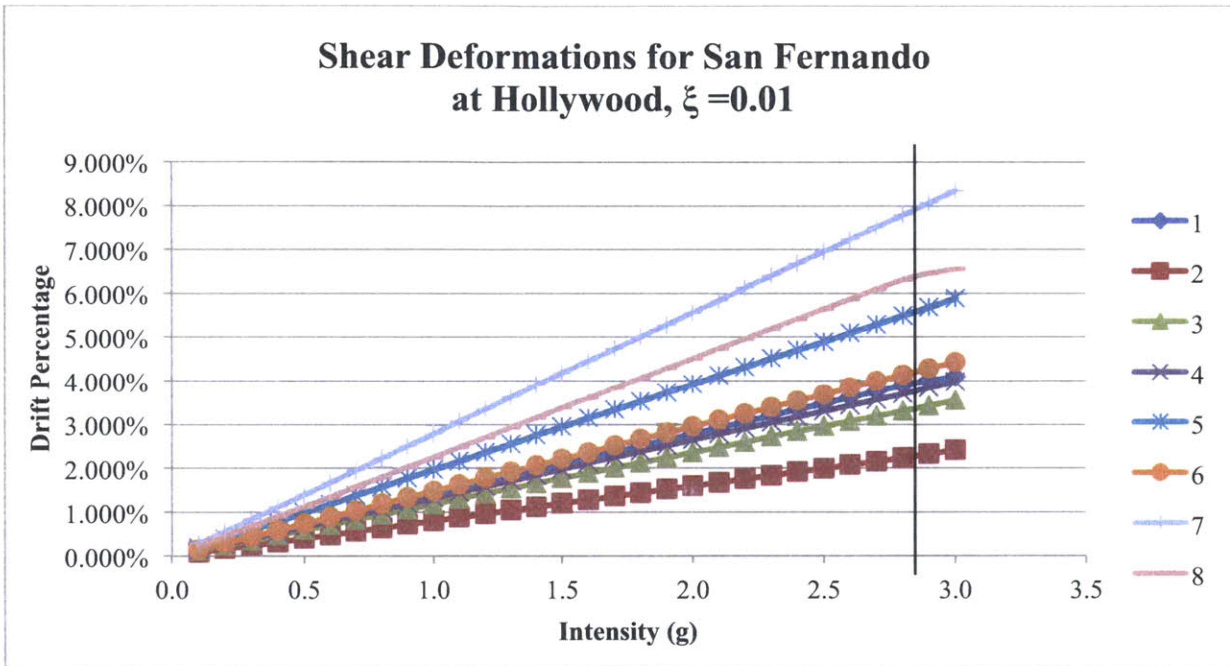


**Figure 23 – Nonlinear Shear Deformations for San Fernando at Hollywood, $\xi$ =0.01**

Lastly, the structure was modeled using a 1% damping ratio. The structure begins to experience the nonlinear behavior at 2.9g, but not in the 7th link. In this case, the link 8$^{th}$ representing the columns on the 8$^{th}$ floor experience the nonlinear behavior. It is more apparent when observing the acceleration in Figure 24. The accelerations of node 8 and 9, which represent the 8$^{th}$ floor and roofline begin to deviate from linearity.

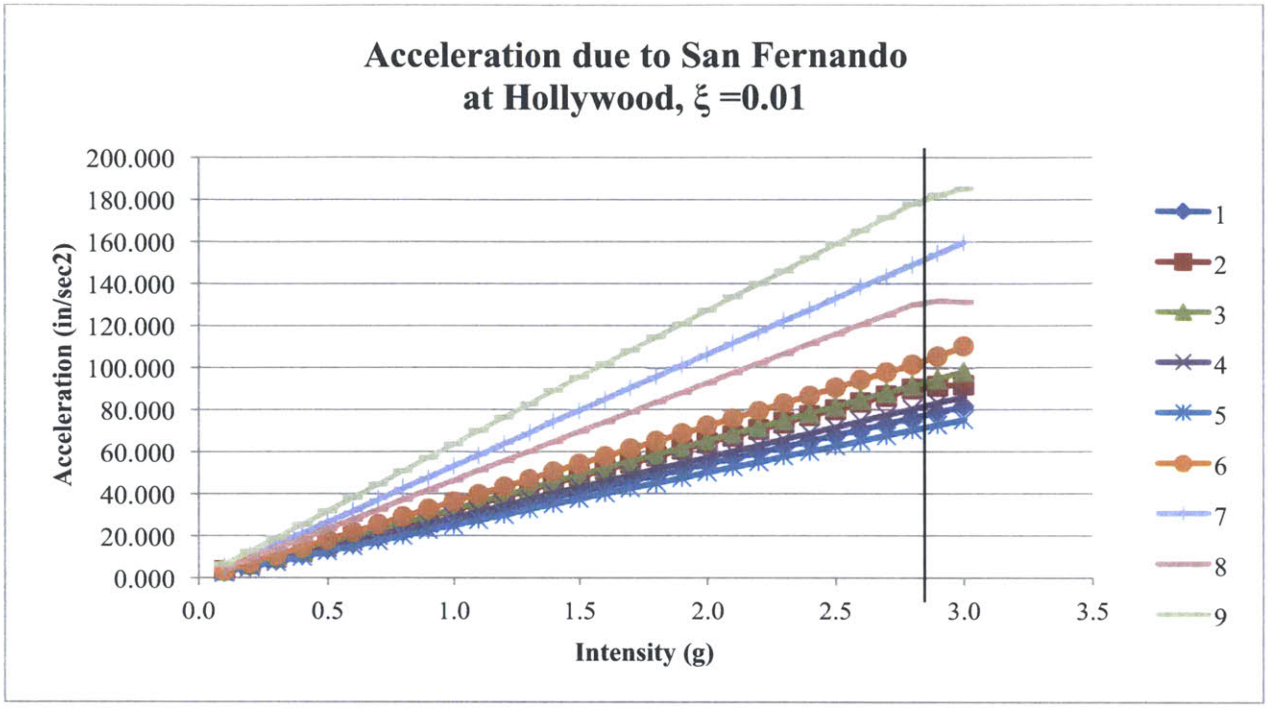


**Figure 24 - Nonlinear Accelerations for San Fernando at Hollywood, ξ =0.01**

As in the first two (2) approaches, the structure continues to perform linearly for earthquakes less than 1.0g.

# 5 Conclusions

This research has concluded based on the assumptions defined in Chapter 2 and Chapter 3 that shear deformations and floor accelerations for reinforced concrete structures can be approximated through linear analysis. The conclusion applies to structures designed according to modern code and is not necessarily applicable to structures built to previous standards, though these results may be applicable to existing structures that may have a similar damping ratio. This hypothesis can only be proven with further research. It is important to not that this model is not perfect and additional work must be done to produce a more accurate representation of reinforced concrete structures. Some of the additional work has been outlined in Section 5.1.

## 5.1 Further Considerations

This research requires further considerations and work. There is a potential to explore additional behaviors, a larger range of damping ratios, more complicated structural types and improvements to existing design techniques.

This research only explored a 2-dimension representation of potential reinforced concrete structure. Additional research can explore a 3-dimension moment resisting frame structure. The six (6) degrees of freedom would provide a more accurate depiction of how the structure would perform under these earthquake scenarios.

The software analysis used in this research, SAP2000, is quite sophisticated. Proper analysis can be difficult. An exploration into different reinforced concrete modeling or the use of different analysis techniques could be noteworthy. Additionally, sensitivity analysis based on the assumptions stated previous in the paper could provide further insight into the accuracy of these results.

Based on this analysis, the weakest portion of the structure was the top tier of the structure where the columns transitioned in sizing. Though not explored, it would be interesting to explore how small design variations could affect the overall performance of the structure. Variations, such as increasing the strength of the top portion of the structure, could bring significant improvements to the structure or might result in more acceleration-induced damage.

This research has the ability to be coupled with the work performed by Pierre Ghisbain, a former doctoral student at the Massachusetts Institute of Technology. In his work, titled Seismic Performance Assessment for Structural Optimization, Ghisbain optimizes a buildings design and performance based on lifetime cost including initial construction costs and maintenance costs associated with earthquake related damage over the life of the structure. His work takes an excellent look at steel structures and leaves the opportunity open to perform the same analysis with reinforced concrete structures.

# 6 References


(1) ACI Committee 318. "Building Code Requirements for Structureal Concrete (ACI318-11)." Farmington Hills: American Concrete Institute, 2011.

(2) American Society of Civil Engineers. "Minimum Design Loads of Buildings and Other Buildings." Reston: American Society of Civil Engineers, 2010.

(3) Ghisbain, Pierre. Seismic Performance Assessment for Structural Optimization. Cambridge: Pierre Ghisbain, 2013.

# 7 Appendix

## 7.1 Earthquake Data

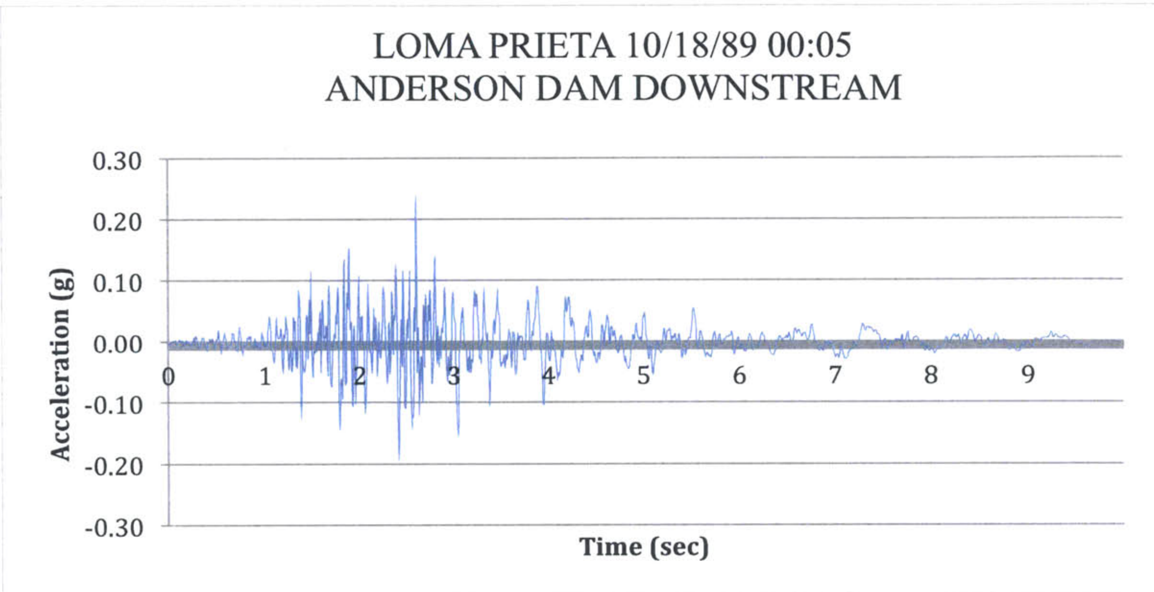


**Figure 25 - Loma Prieta Earthquake at Anderson Dam**

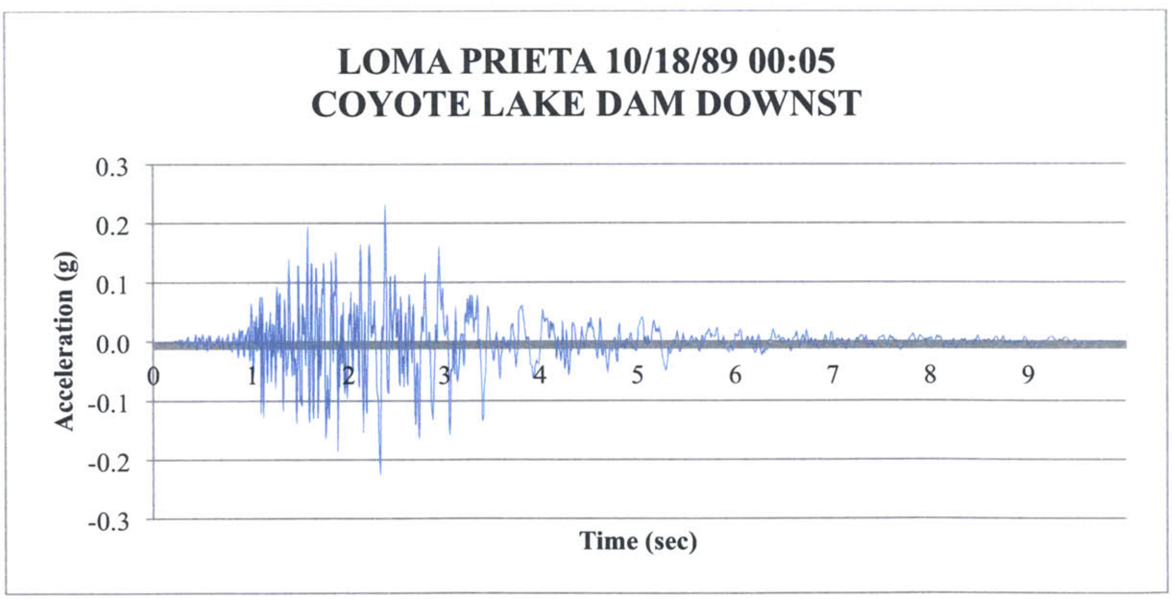


**Figure 26 - Loma Prieta Earthquake at Coyote Lake Dam**

## 7.2 Beam Calculations

This is the beam design for ultimate negative moment that occurs at the beam supports

| Material Properties | | |
|---|---|---|
| $f_c'$ | 4 | ksi |
| $f_y$ | 60 | ksi |

| Beam Dimensions | | |
|---|---|---|
| length, l | 30 | ft |
| height, h | 24 | in |
| width, w | 24 | in |
| concrete cover, cc | 2.5 | in |

| | | | |
|---|---|---|---|
| weight of beam | 0.6 | klf | =(150pcf*h*w) / ($144in^2/ft^2$) |
| Continuous Beam Max Moment | 480 | kip-ft | from SAP Model |
| $J_d$ | 18.81 | in | =0.875*(h-cc) |
| Area Steel | 5.67 | $in^2$ | =($M_{max}$*12in/ft) / (0.9*$J_d$*fy) |
| Area of Steel, $A_{st}$ | 7 | $in^2$ | based on calculated steel area |
| height of compression block, a | 5.15 | in | =($A_{st}$*$f_y$) / (0.85*$f'_c$*w) |
| Nominal Moment, $M_n$ | 662 | kip-ft | =$A_{st}$*$f_y$*(h-cc-(a/2)) / (12in/ft) |
| Ultimate Moment, $M_u$ | 596 | > | 480 |

Beam can support load

This is the beam design for ultimate positive moment that occurs at the beam midspan

| Material Properties | | | |
|---|---|---|---|
| $f_c'$ | 4 | ksi | |
| $f_y$ | 60 | ksi | |

| Beam Dimensions | | | |
|---|---|---|---|
| length, l | 30 | ft | |
| height, h | 24 | in | |
| width, w | 24 | in | |
| concrete cover, cc | 2.5 | in | |
| weight of beam | 0.6 | klf | $=(150pcf*h*w) / (144in^2/ft^2)$ |
| Continuous Beam Max Moment | 240 | kip-ft | from SAP Model |
| $J_d$ | 18.81 | in | =0.875*(h-cc) |
| Area Steel | 2.83 | $in^2$ | $=(M_{max}*12in/ft) / (0.9*J_d*fy)$ |
| Area of Steel, $A_{st}$ | 3 | $in^2$ | based on calculated steel area |
| height of compression block, a | 2.21 | in | $=(A_{st}*f_y) / (0.85*f'_c*w)$ |
| Nominal Moment, $M_n$ | 306 | kip-ft | $=A_{st}*f_y*(h-cc-(a/2)) / (12in/ft)$ |
| Ultimate Moment, $M_u$ | 275 | > | 240 |

Beam can support load

## 7.3 Column Calculations

| Material Properties | | |
|---|---|---|
| $f_c'$ | 4000 | psi |
| $f_y$ | 60000 | psi |
| $A_{st}/A_g$ | 0.04 | ratio |

| | | 12 ext | 34 ext | 56 ext | 78 ext | 12 int | 34 int | 56 int | 78 int | |
|---|---|---|---|---|---|---|---|---|---|---|
| | Pu (kips) | 685 | 487 | 236 | 155 | 1515 | 1138 | 758 | 379 | from SAP |
| | $P_n = P_u / \Phi$ | 761 | 541 | 262 | 172 | 1683 | 1264 | 842 | 421 | |
| | Ag (in$^2$) | 158 | 112 | 54 | 36 | 350 | 263 | 175 | 87 | ACI 10.3.6.1 |
| | Sq. Col. Dim. (in) | 12.6 | 10.6 | 7.4 | 6.0 | 18.7 | 16.2 | 13.2 | 9.4 | =sqrt($A_g$) |
| | Dimension used (in) | 14.0 | 12.0 | 10.0 | 8.0 | 20.0 | 18.0 | 16.0 | 12.0 | |
| | $A_g$ | 196.0 | 144.0 | 100.0 | 64.0 | 400.0 | 324.0 | 256.0 | 144.0 | |
| $A_{bar}$ | $A_{st}$ | 7.84 | 5.76 | 4 | 2.56 | 16 | 12.96 | 10.24 | 5.76 | |
| 1.27 | No.10 | 7 | 5 | 4 | 3 | 13 | 11 | 9 | 5 | |
| 1 | No.9 | 8 | 6 | 4 | 3 | 16 | 13 | 11 | 6 | |
| 0.79 | No.8 | 10 | 8 | 6 | 4 | 21 | 17 | 13 | 8 | |
| 0.6 | No.7 | 14 | 10 | 7 | 5 | 27 | 22 | 18 | 10 | |
| 0.44 | No.6 | 18 | 14 | 10 | 6 | 37 | 30 | 24 | 14 | |

## 7.4 Column Section

**Table 4 - Column Sizes**

| | | Reinforcement | |
|---|---|---|---|
| | Dimensions | No. Bars | Bar Size |
| EXT12 | 14 x 14 | 8 | #9 |
| EXT34 | 12 x 12 | 6 | #9 |
| EXT56 | 10 x 10 | 6 | #8 |
| EXT78 | 8 x 8 | 6 | #6 |
| INT12 | 20 x 20 | 16 | #9 |
| INT34 | 18 x 18 | 14 | #9 |
| INT56 | 16 x 16 | 14 | #8 |
| INT78 | 12 x 12 | 8 | #8 |

## 7.5 Link Deformations | Shear Deformation Percentage

**Table 5 - Link Deformations: San Fernando at Hollywood, ξ =0.05**

| Earthquake Intensity (g) | Link 1 | 2 | 3 | 4 | 5 | 6 | 7 | 8 |
|---|---|---|---|---|---|---|---|---|
| 0.1 | 0.111% | 0.072% | 0.099% | 0.102% | 0.146% | 0.129% | 0.257% | 0.149% |
| 0.2 | 0.222% | 0.144% | 0.199% | 0.205% | 0.292% | 0.258% | 0.514% | 0.298% |
| 0.3 | 0.334% | 0.216% | 0.298% | 0.307% | 0.438% | 0.386% | 0.770% | 0.447% |
| 0.4 | 0.445% | 0.288% | 0.398% | 0.409% | 0.585% | 0.515% | 1.027% | 0.596% |
| 0.5 | 0.556% | 0.359% | 0.497% | 0.512% | 0.731% | 0.644% | 1.284% | 0.744% |
| 0.6 | 0.667% | 0.431% | 0.597% | 0.614% | 0.877% | 0.773% | 1.541% | 0.893% |
| 0.7 | 0.778% | 0.503% | 0.696% | 0.717% | 1.023% | 0.901% | 1.797% | 1.042% |
| 0.8 | 0.889% | 0.575% | 0.795% | 0.819% | 1.169% | 1.030% | 2.054% | 1.191% |
| 0.9 | 1.001% | 0.647% | 0.895% | 0.921% | 1.315% | 1.159% | 2.311% | 1.340% |
| 1 | 1.112% | 0.719% | 0.994% | 1.024% | 1.462% | 1.288% | 2.568% | 1.489% |
| 1.1 | 1.223% | 0.791% | 1.094% | 1.126% | 1.608% | 1.416% | 2.825% | 1.638% |
| 1.2 | 1.334% | 0.863% | 1.193% | 1.228% | 1.754% | 1.545% | 3.081% | 1.787% |
| 1.3 | 1.445% | 0.935% | 1.293% | 1.331% | 1.900% | 1.674% | 3.338% | 1.935% |
| 1.4 | 1.557% | 1.006% | 1.392% | 1.433% | 2.046% | 1.803% | 3.595% | 2.084% |
| 1.5 | 1.668% | 1.078% | 1.491% | 1.536% | 2.192% | 1.932% | 3.852% | 2.233% |
| 1.6 | 1.779% | 1.150% | 1.591% | 1.638% | 2.338% | 2.060% | 4.109% | 2.382% |
| 1.7 | 1.890% | 1.222% | 1.690% | 1.740% | 2.485% | 2.189% | 4.365% | 2.531% |
| 1.8 | 2.001% | 1.294% | 1.790% | 1.843% | 2.631% | 2.318% | 4.622% | 2.680% |
| 1.9 | 2.112% | 1.366% | 1.889% | 1.945% | 2.777% | 2.447% | 4.879% | 2.829% |
| 2.0 | 2.224% | 1.438% | 1.989% | 2.047% | 2.923% | 2.575% | 5.136% | 2.978% |
| 2.1 | 2.335% | 1.510% | 2.088% | 2.150% | 3.069% | 2.704% | 5.392% | 3.126% |
| 2.2 | 2.446% | 1.582% | 2.187% | 2.252% | 3.215% | 2.833% | 5.649% | 3.275% |
| 2.3 | 2.557% | 1.653% | 2.287% | 2.354% | 3.362% | 2.962% | 5.906% | 3.424% |
| 2.4 | 2.668% | 1.725% | 2.386% | 2.457% | 3.508% | 3.091% | 6.163% | 3.573% |
| 2.5 | 2.780% | 1.797% | 2.486% | 2.559% | 3.654% | 3.219% | 6.420% | 3.722% |
| 2.6 | 2.891% | 1.869% | 2.585% | 2.662% | 3.800% | 3.348% | 6.676% | 3.871% |
| 2.7 | 3.002% | 1.941% | 2.685% | 2.764% | 3.946% | 3.477% | 6.933% | 4.020% |
| 2.8 | 3.113% | 2.013% | 2.784% | 2.866% | 4.092% | 3.606% | 7.190% | 4.169% |
| 2.9 | 3.224% | 2.085% | 2.883% | 2.969% | 4.238% | 3.734% | 7.447% | 4.317% |
| 3.0 | 3.335% | 2.157% | 2.983% | 3.071% | 4.385% | 3.863% | 7.703% | 4.466% |
| 3.1 | 3.447% | 2.229% | 3.082% | 3.173% | 4.525% | 3.982% | 7.960% | 4.615% |
| 3.2 | 3.558% | 2.300% | 3.181% | 3.268% | 4.642% | 4.071% | 8.218% | 4.756% |
| 3.3 | 3.669% | 2.372% | 3.278% | 3.358% | 4.762% | 4.146% | 8.490% | 4.887% |
| 3.4 | 3.781% | 2.444% | 3.372% | 3.441% | 4.906% | 4.206% | 8.905% | 5.010% |
| 3.5 | 3.892% | 2.515% | 3.465% | 3.520% | 5.050% | 4.301% | 9.599% | 5.125% |
| 3.6 | 4.005% | 2.586% | 3.555% | 3.594% | 5.194% | 4.388% | 10.362% | 5.232% |
| 3.7 | 4.124% | 2.659% | 3.645% | 3.666% | 5.339% | 4.470% | 11.253% | 5.329% |
| 3.8 | 4.245% | 2.733% | 3.734% | 3.735% | 5.483% | 4.545% | 12.235% | 5.416% |
| 3.9 | 4.376% | 2.826% | 3.811% | 3.798% | 5.627% | 4.655% | 13.297% | 5.490% |
| 4.0 | 4.516% | 2.925% | 3.883% | 3.885% | 5.772% | 4.775% | 14.455% | 5.554% |
| 4.1 | 4.662% | 3.025% | 3.977% | 3.987% | 5.916% | 4.894% | 15.695% | 5.611% |
| 4.2 | 4.811% | 3.126% | 4.072% | 4.086% | 6.060% | 5.013% | 17.011% | 5.652% |

| | | | | | | | | |
|---|---|---|---|---|---|---|---|---|
| 4.3 | 4.965% | 3.231% | 4.170% | 4.187% | 6.199% | 5.130% | 18.367% | 5.693% |
| 4.4 | 5.122% | 3.336% | 4.269% | 4.286% | 6.335% | 5.245% | 19.794% | 5.719% |
| 4.5 | 5.277% | 3.444% | 4.369% | 4.385% | 6.471% | 5.358% | 21.215% | 5.748% |
| 4.6 | 5.425% | 3.548% | 4.467% | 4.481% | 6.606% | 5.470% | 22.594% | 5.772% |
| 4.7 | 5.502% | 3.658% | 4.564% | 4.575% | 6.742% | 5.578% | 23.929% | 5.798% |
| 4.8 | 5.503% | 3.784% | 4.658% | 4.668% | 6.877% | 5.684% | 25.256% | 5.825% |
| 4.9 | 5.504% | 3.900% | 4.745% | 4.757% | 7.012% | 5.787% | 26.544% | 5.854% |
| 5.0 | 5.504% | 4.022% | 4.831% | 4.848% | 7.140% | 5.879% | 30.117% | 88.523% |

**Table 6 - Link Deformations: Loma Prieta at Anderson Dam, $\xi$ =0.05**

| Earthquake Intensity (g) | Link 1 | 2 | 3 | 4 | 5 | 6 | 7 | 8 |
|---|---|---|---|---|---|---|---|---|
| 0.1 | 0.104% | 0.064% | 0.081% | 0.079% | 0.117% | 0.111% | 0.222% | 0.122% |
| 0.2 | 0.208% | 0.127% | 0.162% | 0.159% | 0.233% | 0.222% | 0.443% | 0.243% |
| 0.3 | 0.311% | 0.191% | 0.243% | 0.238% | 0.350% | 0.333% | 0.665% | 0.365% |
| 0.4 | 0.415% | 0.255% | 0.325% | 0.318% | 0.466% | 0.443% | 0.887% | 0.486% |
| 0.5 | 0.519% | 0.318% | 0.406% | 0.397% | 0.583% | 0.554% | 1.109% | 0.608% |
| 0.6 | 0.623% | 0.382% | 0.487% | 0.477% | 0.699% | 0.665% | 1.330% | 0.729% |
| 0.7 | 0.726% | 0.445% | 0.568% | 0.556% | 0.816% | 0.776% | 1.552% | 0.851% |
| 0.8 | 0.830% | 0.509% | 0.649% | 0.635% | 0.932% | 0.887% | 1.774% | 0.972% |
| 0.9 | 0.934% | 0.573% | 0.730% | 0.715% | 1.049% | 0.998% | 1.996% | 1.094% |
| 1 | 1.038% | 0.636% | 0.812% | 0.794% | 1.165% | 1.109% | 2.217% | 1.215% |

**Table 7 - Link Deformations: Loma Prieta at Coyote Lake Dam, $\xi$ =0.05**

| Earthquake Intensity (g) | Link 1 | 2 | 3 | 4 | 5 | 6 | 7 | 8 |
|---|---|---|---|---|---|---|---|---|
| 0.1 | 0.231% | 0.130% | 0.168% | 0.165% | 0.242% | 0.221% | 0.426% | 0.228% |
| 0.2 | 0.462% | 0.260% | 0.336% | 0.329% | 0.484% | 0.443% | 0.852% | 0.456% |
| 0.3 | 0.694% | 0.391% | 0.504% | 0.494% | 0.726% | 0.664% | 1.277% | 0.684% |
| 0.4 | 0.925% | 0.521% | 0.672% | 0.659% | 0.968% | 0.885% | 1.703% | 0.912% |
| 0.5 | 1.156% | 0.651% | 0.840% | 0.824% | 1.211% | 1.107% | 2.129% | 1.140% |
| 0.6 | 1.387% | 0.781% | 1.007% | 0.988% | 1.453% | 1.328% | 2.555% | 1.368% |
| 0.7 | 1.619% | 0.912% | 1.175% | 1.153% | 1.695% | 1.549% | 2.981% | 1.596% |
| 0.8 | 1.850% | 1.042% | 1.343% | 1.318% | 1.937% | 1.771% | 3.406% | 1.824% |
| 0.9 | 2.081% | 1.172% | 1.511% | 1.483% | 2.179% | 1.992% | 3.832% | 2.052% |
| 1 | 2.312% | 1.302% | 1.679% | 1.647% | 2.421% | 2.213% | 4.258% | 2.280% |

## Table 8 - Link Deformations: San Fernando at Hollywood, $\xi = 0.03$

| Earthquake Intensity (g) | Link 1 | 2 | 3 | 4 | 5 | 6 | 7 | 8 |
|---|---|---|---|---|---|---|---|---|
| 0.1 | 0.121% | 0.075% | 0.105% | 0.109% | 0.164% | 0.136% | 0.255% | 0.149% |
| 0.2 | 0.243% | 0.150% | 0.211% | 0.218% | 0.328% | 0.273% | 0.510% | 0.299% |
| 0.3 | 0.364% | 0.225% | 0.316% | 0.328% | 0.493% | 0.409% | 0.765% | 0.448% |
| 0.4 | 0.485% | 0.300% | 0.421% | 0.437% | 0.657% | 0.545% | 1.021% | 0.598% |
| 0.5 | 0.606% | 0.375% | 0.527% | 0.546% | 0.821% | 0.681% | 1.276% | 0.747% |
| 0.6 | 0.728% | 0.450% | 0.632% | 0.655% | 0.985% | 0.818% | 1.531% | 0.897% |
| 0.7 | 0.849% | 0.525% | 0.737% | 0.765% | 1.150% | 0.954% | 1.786% | 1.046% |
| 0.8 | 0.970% | 0.600% | 0.843% | 0.874% | 1.314% | 1.090% | 2.041% | 1.196% |
| 0.9 | 1.091% | 0.675% | 0.948% | 0.983% | 1.478% | 1.226% | 2.296% | 1.345% |
| 1.0 | 1.213% | 0.750% | 1.053% | 1.092% | 1.642% | 1.363% | 2.551% | 1.495% |
| 1.1 | 1.334% | 0.825% | 1.159% | 1.202% | 1.807% | 1.499% | 2.806% | 1.644% |
| 1.2 | 1.455% | 0.899% | 1.264% | 1.311% | 1.971% | 1.635% | 3.062% | 1.794% |
| 1.3 | 1.576% | 0.974% | 1.370% | 1.420% | 2.135% | 1.771% | 3.317% | 1.943% |
| 1.4 | 1.698% | 1.049% | 1.475% | 1.529% | 2.299% | 1.908% | 3.572% | 2.093% |
| 1.5 | 1.819% | 1.124% | 1.580% | 1.638% | 2.464% | 2.044% | 3.827% | 2.242% |
| 1.6 | 1.940% | 1.199% | 1.686% | 1.748% | 2.628% | 2.180% | 4.082% | 2.392% |
| 1.7 | 2.061% | 1.274% | 1.791% | 1.857% | 2.792% | 2.317% | 4.337% | 2.541% |
| 1.8 | 2.183% | 1.349% | 1.896% | 1.966% | 2.956% | 2.453% | 4.592% | 2.691% |
| 1.9 | 2.304% | 1.424% | 2.002% | 2.075% | 3.121% | 2.589% | 4.847% | 2.840% |
| 2.0 | 2.425% | 1.499% | 2.107% | 2.185% | 3.285% | 2.725% | 5.103% | 2.990% |
| 2.1 | 2.546% | 1.574% | 2.212% | 2.294% | 3.449% | 2.862% | 5.358% | 3.139% |
| 2.2 | 2.668% | 1.649% | 2.318% | 2.403% | 3.613% | 2.998% | 5.613% | 3.288% |
| 2.3 | 2.789% | 1.724% | 2.423% | 2.512% | 3.778% | 3.134% | 5.868% | 3.438% |
| 2.4 | 2.910% | 1.799% | 2.528% | 2.622% | 3.942% | 3.270% | 6.123% | 3.587% |
| 2.5 | 3.031% | 1.874% | 2.634% | 2.731% | 4.106% | 3.407% | 6.378% | 3.737% |
| 2.6 | 3.153% | 1.949% | 2.739% | 2.840% | 4.270% | 3.543% | 6.633% | 3.886% |
| 2.7 | 3.274% | 2.024% | 2.844% | 2.949% | 4.434% | 3.679% | 6.888% | 4.036% |
| 2.8 | 3.395% | 2.099% | 2.950% | 3.059% | 4.599% | 3.815% | 7.144% | 4.185% |
| 2.9 | 3.516% | 2.174% | 3.055% | 3.168% | 4.763% | 3.952% | 7.399% | 4.335% |
| 3.0 | 3.638% | 2.249% | 3.160% | 3.277% | 4.927% | 4.088% | 7.654% | 4.484% |
| 3.1 | 3.759% | 2.324% | 3.266% | 3.386% | 5.091% | 4.206% | 7.909% | 4.634% |
| 3.2 | 3.881% | 2.399% | 3.371% | 3.495% | 5.256% | 4.291% | 8.173% | 4.778% |
| 3.3 | 4.009% | 2.479% | 3.480% | 3.605% | 5.420% | 4.360% | 8.678% | 4.919% |
| 3.4 | 4.140% | 2.561% | 3.589% | 3.714% | 5.584% | 4.463% | 9.520% | 5.069% |
| 3.5 | 4.270% | 2.646% | 3.698% | 3.823% | 5.748% | 4.594% | 10.478% | 5.212% |
| 3.6 | 4.407% | 2.732% | 3.806% | 3.932% | 5.913% | 4.725% | 11.564% | 5.343% |
| 3.7 | 4.552% | 2.829% | 3.909% | 4.042% | 6.077% | 4.856% | 12.757% | 5.460% |
| 3.8 | 4.700% | 2.947% | 3.997% | 4.151% | 6.241% | 4.988% | 14.040% | 5.561% |
| 3.9 | 4.850% | 3.067% | 4.082% | 4.260% | 6.405% | 5.119% | 15.425% | 5.646% |
| 4.0 | 4.999% | 3.188% | 4.165% | 4.366% | 6.565% | 5.248% | 16.863% | 5.717% |

**Table 9 - Link Deformations: Loma Prieta at Anderson Dam, $\xi$ =0.03**

| Earthquake Intensity (g) \ Link | 1 | 2 | 3 | 4 | 5 | 6 | 7 | 8 |
|---|---|---|---|---|---|---|---|---|
| 0.1 | 0.122% | 0.066% | 0.085% | 0.085% | 0.122% | 0.111% | 0.228% | 0.131% |
| 0.2 | 0.245% | 0.132% | 0.170% | 0.170% | 0.243% | 0.223% | 0.457% | 0.263% |
| 0.3 | 0.367% | 0.198% | 0.255% | 0.255% | 0.365% | 0.334% | 0.685% | 0.394% |
| 0.4 | 0.490% | 0.264% | 0.339% | 0.340% | 0.487% | 0.446% | 0.914% | 0.526% |
| 0.5 | 0.612% | 0.330% | 0.424% | 0.425% | 0.609% | 0.557% | 1.142% | 0.657% |
| 0.6 | 0.734% | 0.396% | 0.509% | 0.510% | 0.730% | 0.668% | 1.371% | 0.788% |
| 0.7 | 0.857% | 0.462% | 0.594% | 0.595% | 0.852% | 0.780% | 1.599% | 0.920% |
| 0.8 | 0.979% | 0.528% | 0.679% | 0.680% | 0.974% | 0.891% | 1.828% | 1.051% |
| 0.9 | 1.102% | 0.594% | 0.764% | 0.765% | 1.095% | 1.002% | 2.056% | 1.183% |
| 1 | 1.224% | 0.660% | 0.848% | 0.850% | 1.217% | 1.114% | 2.285% | 1.314% |

**Table 10 - Link Deformations: Loma Prieta at Coyote Lake Dam, $\xi$ =0.03**

| Earthquake Intensity (g) \ Link | 1 | 2 | 3 | 4 | 5 | 6 | 7 | 8 |
|---|---|---|---|---|---|---|---|---|
| 0.1 | 0.302% | 0.171% | 0.205% | 0.208% | 0.309% | 0.287% | 0.571% | 0.314% |
| 0.2 | 0.604% | 0.342% | 0.411% | 0.416% | 0.618% | 0.575% | 1.142% | 0.629% |
| 0.3 | 0.907% | 0.513% | 0.616% | 0.623% | 0.927% | 0.863% | 1.712% | 0.943% |
| 0.4 | 1.209% | 0.684% | 0.822% | 0.831% | 1.236% | 1.150% | 2.283% | 1.257% |
| 0.5 | 1.511% | 0.855% | 1.027% | 1.039% | 1.545% | 1.438% | 2.854% | 1.571% |
| 0.6 | 1.813% | 1.026% | 1.232% | 1.247% | 1.854% | 1.725% | 3.425% | 1.886% |
| 0.7 | 2.115% | 1.197% | 1.438% | 1.455% | 2.163% | 2.013% | 3.995% | 2.200% |
| 0.8 | 2.417% | 1.368% | 1.643% | 1.663% | 2.471% | 2.300% | 4.566% | 2.514% |
| 0.9 | 2.720% | 1.539% | 1.848% | 1.871% | 2.780% | 2.588% | 5.137% | 2.829% |
| 1 | 3.022% | 1.710% | 2.054% | 2.078% | 3.089% | 2.875% | 5.708% | 3.143% |

## Table 11 - Link Deformations: San Fernando at Hollywood, $\xi$ =0.01

| Earthquake Intensity (g) | Link 1 | 2 | 3 | 4 | 5 | 6 | 7 | 8 |
|---|---|---|---|---|---|---|---|---|
| 0.1 | 0.139% | 0.080% | 0.118% | 0.132% | 0.196% | 0.147% | 0.278% | 0.226% |
| 0.2 | 0.278% | 0.159% | 0.236% | 0.264% | 0.392% | 0.295% | 0.556% | 0.451% |
| 0.3 | 0.417% | 0.239% | 0.353% | 0.396% | 0.587% | 0.442% | 0.835% | 0.677% |
| 0.4 | 0.556% | 0.319% | 0.471% | 0.528% | 0.783% | 0.590% | 1.113% | 0.902% |
| 0.5 | 0.695% | 0.399% | 0.589% | 0.660% | 0.979% | 0.737% | 1.391% | 1.128% |
| 0.6 | 0.834% | 0.478% | 0.707% | 0.792% | 1.175% | 0.884% | 1.669% | 1.354% |
| 0.7 | 0.973% | 0.558% | 0.825% | 0.924% | 1.371% | 1.032% | 1.948% | 1.579% |
| 0.8 | 1.112% | 0.638% | 0.942% | 1.056% | 1.566% | 1.179% | 2.226% | 1.805% |
| 0.9 | 1.251% | 0.717% | 1.060% | 1.188% | 1.762% | 1.326% | 2.504% | 2.031% |
| 1.0 | 1.390% | 0.797% | 1.178% | 1.320% | 1.958% | 1.474% | 2.782% | 2.256% |
| 1.1 | 1.529% | 0.877% | 1.296% | 1.452% | 2.154% | 1.621% | 3.060% | 2.482% |
| 1.2 | 1.668% | 0.956% | 1.414% | 1.585% | 2.349% | 1.769% | 3.339% | 2.707% |
| 1.3 | 1.807% | 1.036% | 1.531% | 1.717% | 2.545% | 1.916% | 3.617% | 2.933% |
| 1.4 | 1.946% | 1.116% | 1.649% | 1.849% | 2.741% | 2.063% | 3.895% | 3.159% |
| 1.5 | 2.085% | 1.196% | 1.767% | 1.981% | 2.937% | 2.211% | 4.173% | 3.384% |
| 1.6 | 2.225% | 1.275% | 1.885% | 2.113% | 3.133% | 2.358% | 4.451% | 3.610% |
| 1.7 | 2.364% | 1.355% | 2.003% | 2.245% | 3.328% | 2.506% | 4.730% | 3.835% |
| 1.8 | 2.503% | 1.435% | 2.120% | 2.377% | 3.524% | 2.653% | 5.008% | 4.061% |
| 1.9 | 2.642% | 1.514% | 2.238% | 2.509% | 3.720% | 2.800% | 5.286% | 4.287% |
| 2.0 | 2.781% | 1.594% | 2.356% | 2.641% | 3.916% | 2.948% | 5.564% | 4.512% |
| 2.1 | 2.920% | 1.674% | 2.474% | 2.773% | 4.112% | 3.095% | 5.843% | 4.738% |
| 2.2 | 3.059% | 1.753% | 2.592% | 2.905% | 4.307% | 3.243% | 6.121% | 4.963% |
| 2.3 | 3.198% | 1.833% | 2.709% | 3.037% | 4.503% | 3.390% | 6.399% | 5.189% |
| 2.4 | 3.337% | 1.913% | 2.827% | 3.169% | 4.699% | 3.537% | 6.677% | 5.415% |
| 2.5 | 3.476% | 1.993% | 2.945% | 3.301% | 4.895% | 3.685% | 6.955% | 5.640% |
| 2.6 | 3.615% | 2.072% | 3.063% | 3.433% | 5.090% | 3.832% | 7.234% | 5.866% |
| 2.7 | 3.754% | 2.152% | 3.181% | 3.565% | 5.286% | 3.979% | 7.512% | 6.092% |
| 2.8 | 3.893% | 2.232% | 3.298% | 3.697% | 5.482% | 4.127% | 7.790% | 6.317% |
| 2.9 | 4.001% | 2.318% | 3.421% | 3.833% | 5.678% | 4.274% | 8.067% | 6.458% |
| 3.0 | 4.093% | 2.407% | 3.546% | 3.971% | 5.874% | 4.422% | 8.349% | 6.555% |

**Table 12 - Link Deformations: Loma Prieta at Anderson Dam, $\xi$ =0.01**

| Earthquake Intensity (g) | Link 1 | 2 | 3 | 4 | 5 | 6 | 7 | 8 |
|---|---|---|---|---|---|---|---|---|
| 0.1 | 0.157% | 0.089% | 0.110% | 0.107% | 0.157% | 0.129% | 0.312% | 0.197% |
| 0.2 | 0.315% | 0.179% | 0.221% | 0.215% | 0.313% | 0.259% | 0.624% | 0.394% |
| 0.3 | 0.472% | 0.268% | 0.331% | 0.322% | 0.470% | 0.388% | 0.935% | 0.591% |
| 0.4 | 0.629% | 0.357% | 0.441% | 0.429% | 0.627% | 0.518% | 1.247% | 0.789% |
| 0.5 | 0.787% | 0.446% | 0.551% | 0.537% | 0.783% | 0.647% | 1.559% | 0.986% |
| 0.6 | 0.944% | 0.536% | 0.662% | 0.644% | 0.940% | 0.777% | 1.871% | 1.183% |
| 0.7 | 1.101% | 0.625% | 0.772% | 0.751% | 1.097% | 0.906% | 2.182% | 1.380% |
| 0.8 | 1.259% | 0.714% | 0.882% | 0.859% | 1.254% | 1.036% | 2.494% | 1.577% |
| 0.9 | 1.416% | 0.804% | 0.993% | 0.966% | 1.410% | 1.165% | 2.806% | 1.774% |
| 1 | 1.573% | 0.893% | 1.103% | 1.073% | 1.567% | 1.295% | 3.118% | 1.972% |

**Table 13 - Link Deformations: Loma Prieta at Coyote Lake Dam, $\xi$ =0.01**

| Earthquake Intensity (g) | Link 1 | 2 | 3 | 4 | 5 | 6 | 7 | 8 |
|---|---|---|---|---|---|---|---|---|
| 0.1 | 0.451% | 0.262% | 0.314% | 0.292% | 0.447% | 0.434% | 0.905% | 0.516% |
| 0.2 | 0.902% | 0.524% | 0.628% | 0.583% | 0.894% | 0.868% | 1.810% | 1.032% |
| 0.3 | 1.353% | 0.785% | 0.942% | 0.875% | 1.340% | 1.302% | 2.715% | 1.549% |
| 0.4 | 1.805% | 1.047% | 1.257% | 1.166% | 1.787% | 1.735% | 3.621% | 2.065% |
| 0.5 | 2.256% | 1.309% | 1.571% | 1.458% | 2.234% | 2.169% | 4.526% | 2.581% |
| 0.6 | 2.707% | 1.571% | 1.885% | 1.750% | 2.681% | 2.603% | 5.431% | 3.097% |
| 0.7 | 3.158% | 1.832% | 2.199% | 2.041% | 3.127% | 3.037% | 6.336% | 3.613% |
| 0.8 | 3.609% | 2.094% | 2.513% | 2.333% | 3.574% | 3.471% | 7.241% | 4.130% |
| 0.9 | 4.032% | 2.349% | 2.827% | 2.612% | 4.018% | 3.880% | 8.201% | 4.606% |
| 1 | 4.283% | 2.535% | 3.095% | 2.888% | 4.404% | 4.070% | 9.782% | 4.787% |

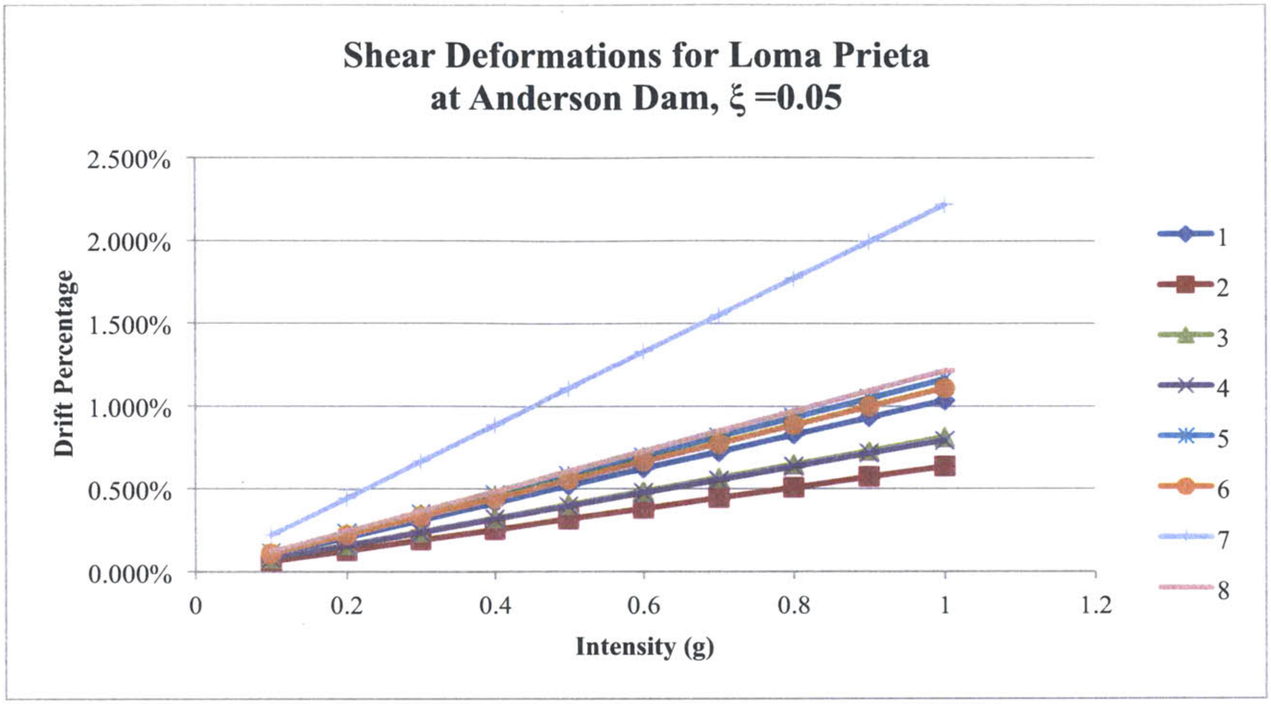


**Figure 27 - Nonlinear Shear Deformations for Loma Prieta at Anderson Dam**

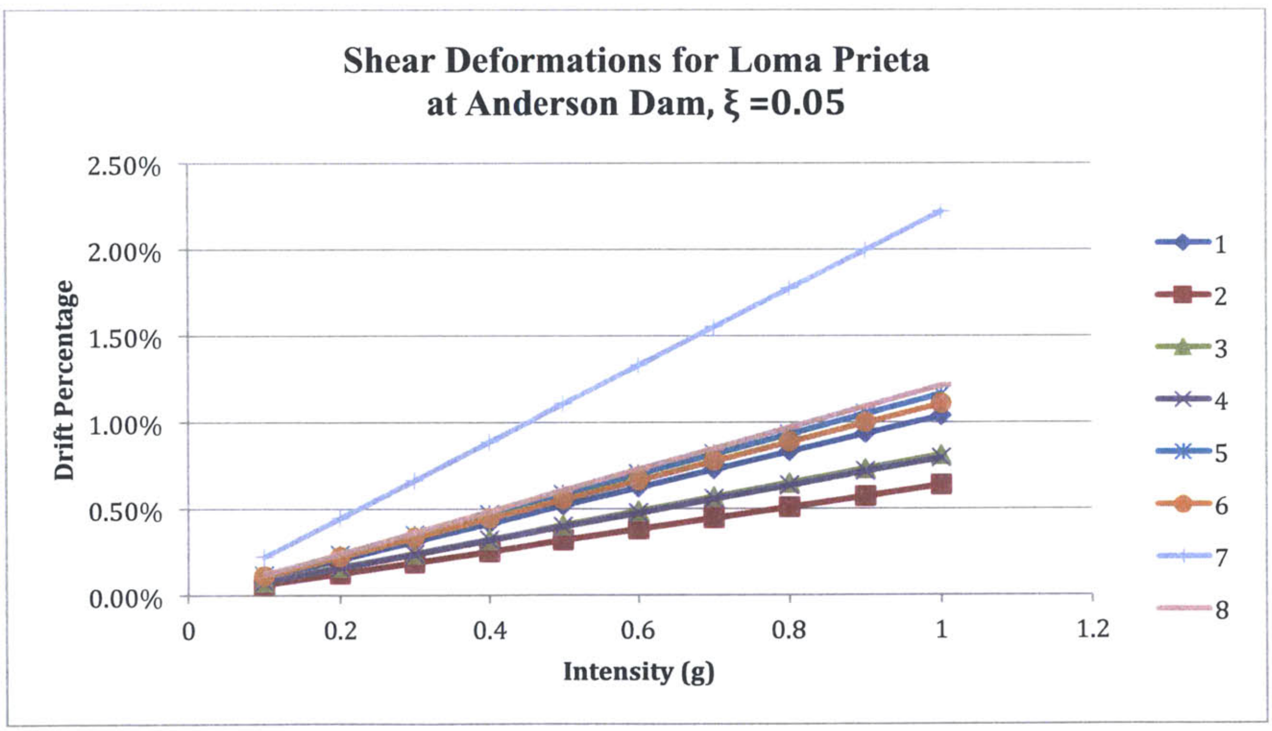


**Figure 28 - Linear Shear Deformations for Loma Prieta at Anderson Dam**

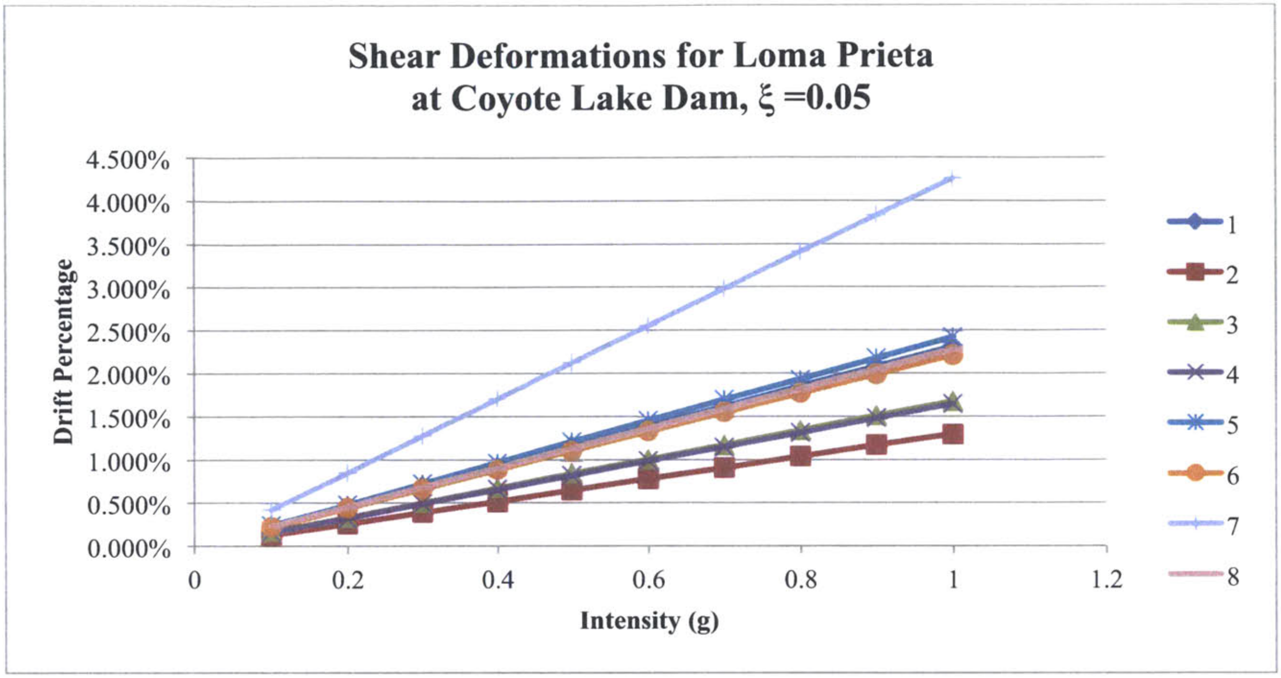


**Figure 29 - Nonlinear Shear Deformations for Loma Prieta at Coyote Lake Dam**

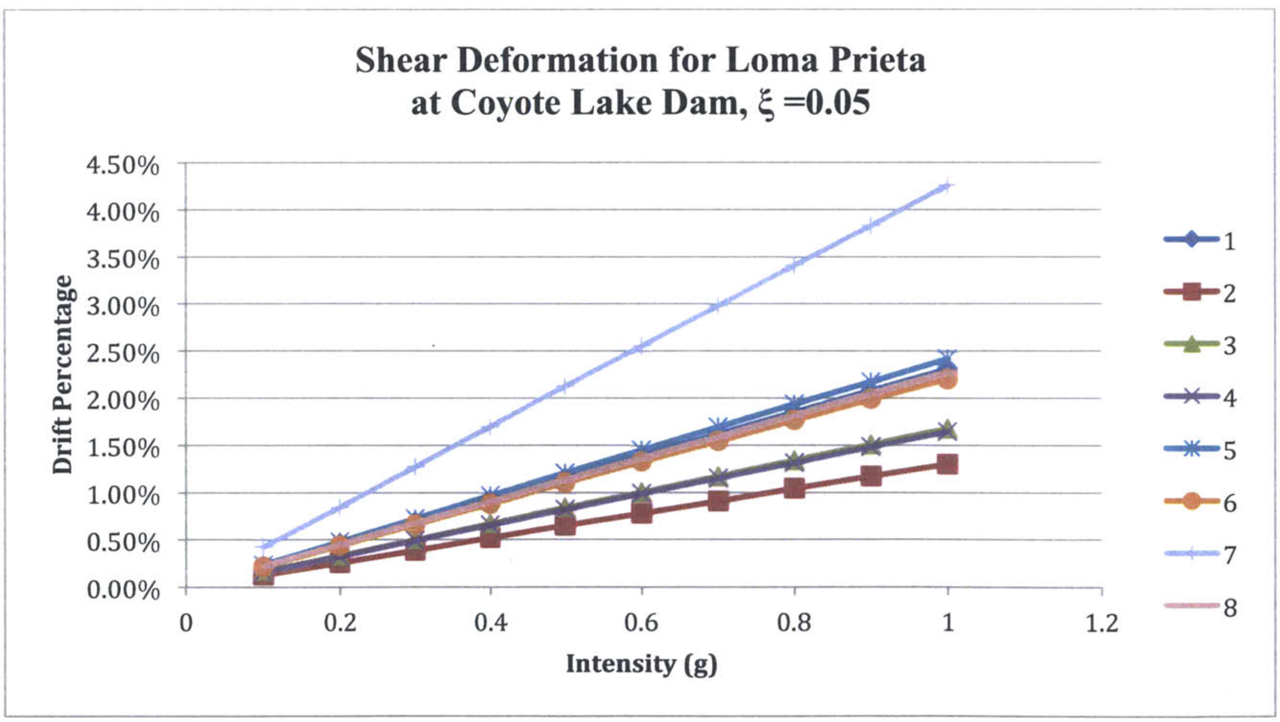


**Figure 30 - Linear Shear Deformations for Loma Prieta at Coyote Lake Dam**

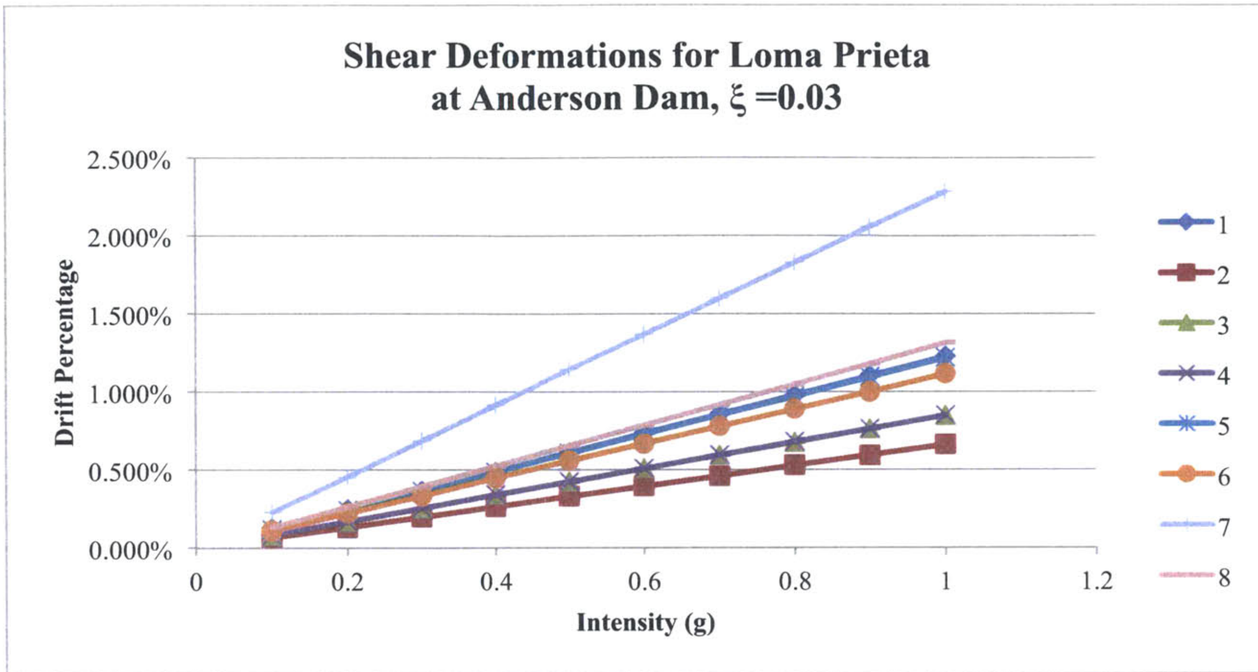


**Figure 31 - Nonlinear Shear Deformations for Loma Prieta at Anderson Dam, ξ =0.03**

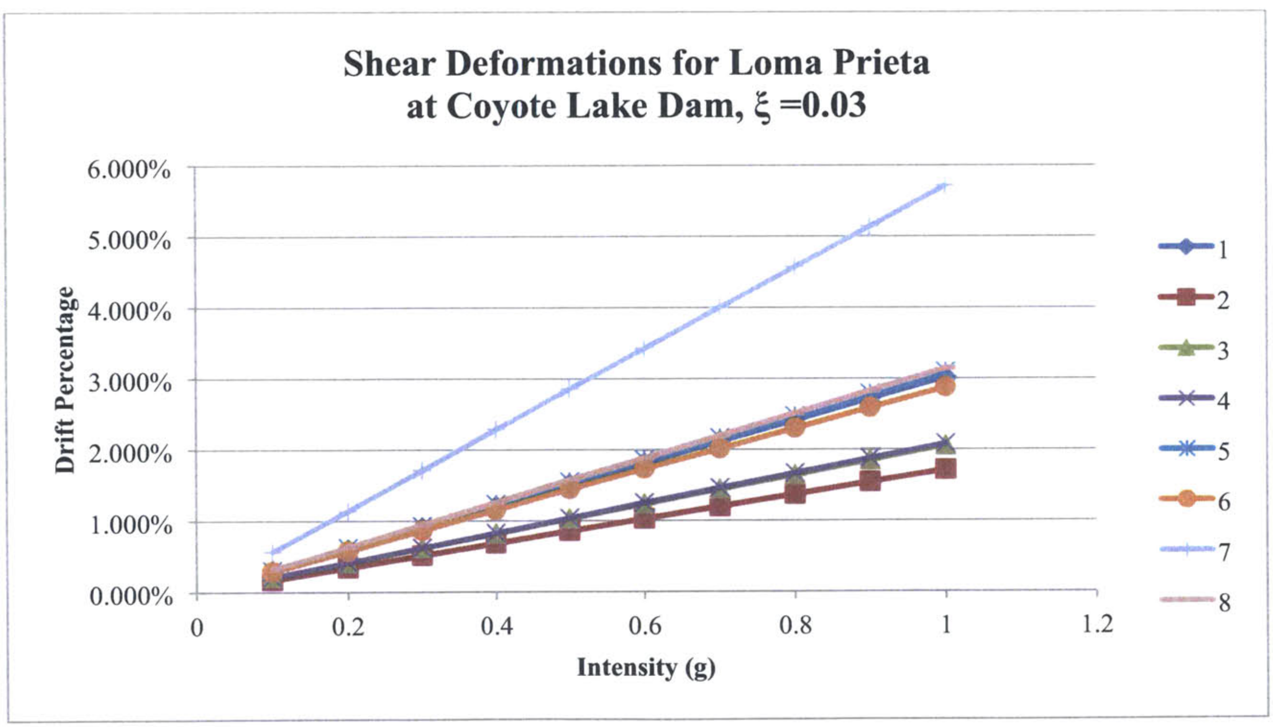


**Figure 32 - Nonlinear Shear Deformations for Loma Prieta at Coyote Lake Dam, ξ =0.03**

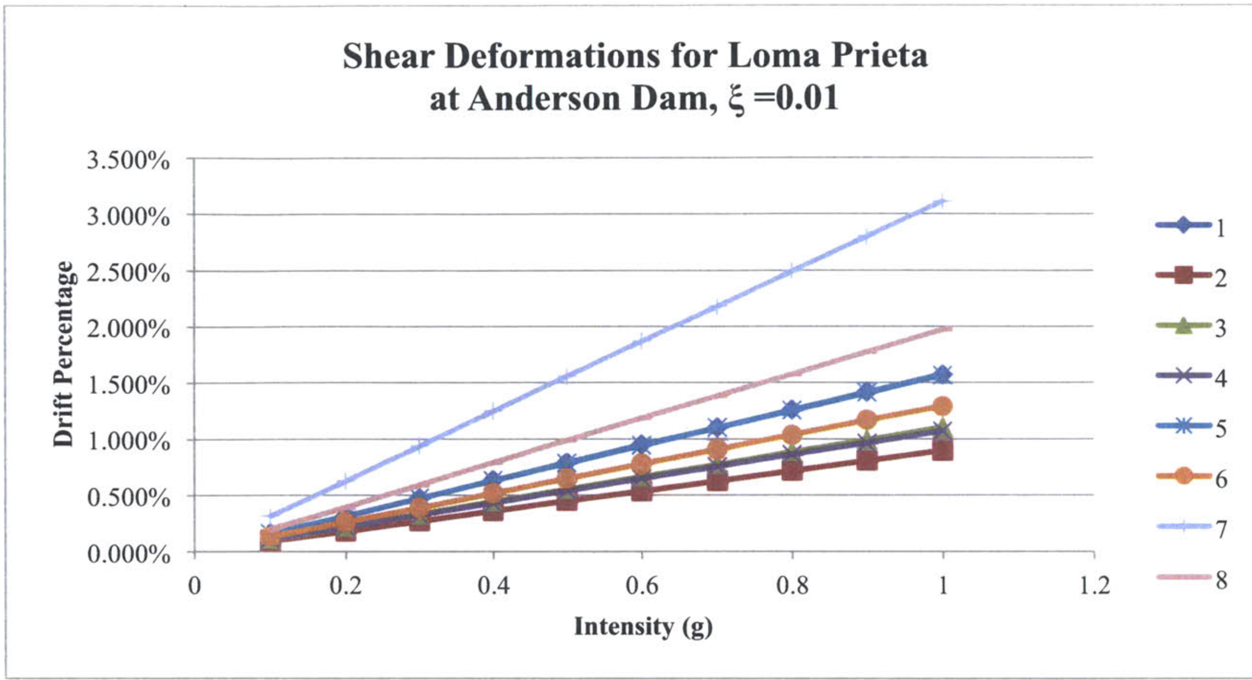


**Figure 33 - Nonlinear Shear Deformations for Loma Prieta at Anderson Dam, ξ =0.01**

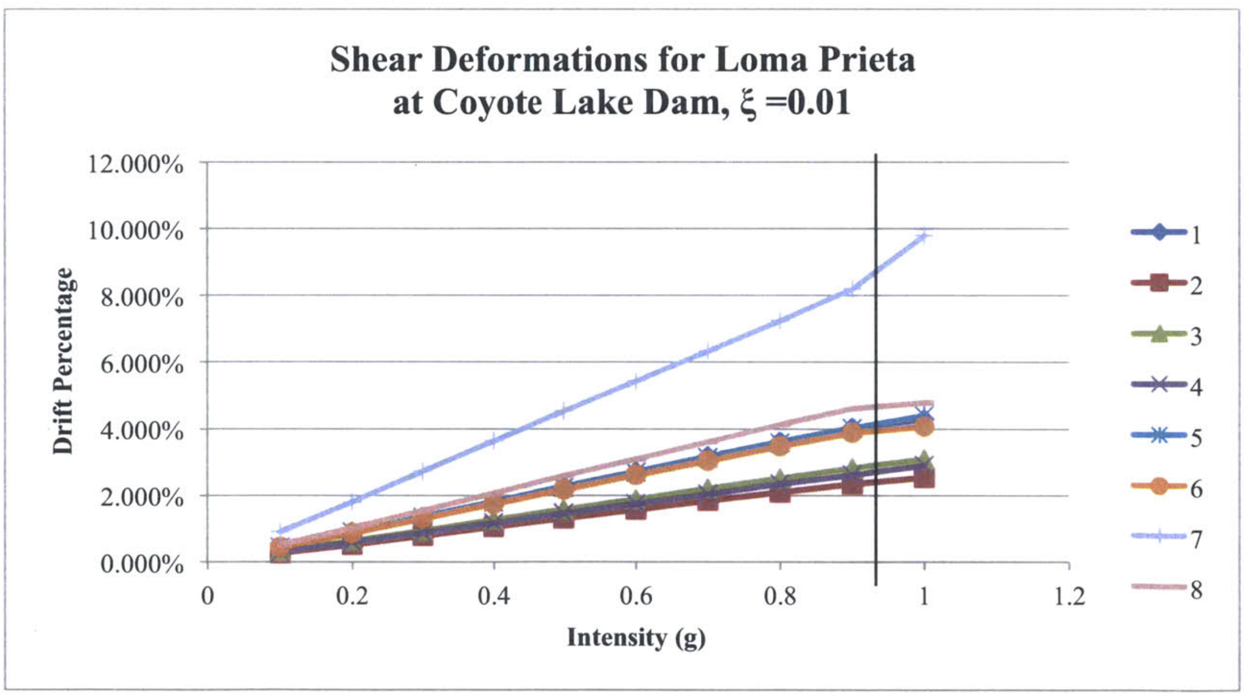


**Figure 34 - Nonlinear Shear Deformations for Loma Prieta at Coyote Lake Dam, ξ =0.01**

# 7.6 Node Accelerations

**Table 14 - Node Accelerations: San Fernando at Hollywood, $\xi$ =0.05**

| Earthquake Intensity (g) | Link 1 | 2 | 3 | 4 | 5 | 6 | 7 | 8 | 9 |
|---|---|---|---|---|---|---|---|---|---|
| 0.1 | 2.715 | 1.732 | 1.799 | 1.652 | 1.561 | 1.952 | 2.758 | 2.892 | 4.237 |
| 0.2 | 5.430 | 3.465 | 3.599 | 3.305 | 3.122 | 3.905 | 5.516 | 5.785 | 8.475 |
| 0.3 | 8.144 | 5.197 | 5.398 | 4.957 | 4.683 | 5.857 | 8.274 | 8.678 | 12.712 |
| 0.4 | 10.859 | 6.929 | 7.197 | 6.609 | 6.244 | 7.810 | 11.032 | 11.570 | 16.950 |
| 0.5 | 13.574 | 8.662 | 8.997 | 8.261 | 7.805 | 9.762 | 13.790 | 14.463 | 21.187 |
| 0.6 | 16.289 | 10.394 | 10.796 | 9.914 | 9.366 | 11.714 | 16.548 | 17.355 | 25.425 |
| 0.7 | 19.004 | 12.126 | 12.595 | 11.566 | 10.927 | 13.667 | 19.307 | 20.248 | 29.662 |
| 0.8 | 21.718 | 13.859 | 14.394 | 13.218 | 12.488 | 15.619 | 22.065 | 23.140 | 33.900 |
| 0.9 | 24.433 | 15.591 | 16.194 | 14.871 | 14.049 | 17.571 | 24.823 | 26.033 | 38.138 |
| 1.0 | 27.148 | 17.324 | 17.993 | 16.523 | 15.610 | 19.524 | 27.581 | 28.925 | 42.375 |
| 1.1 | 29.863 | 19.056 | 19.792 | 18.175 | 17.171 | 21.476 | 30.339 | 31.818 | 46.612 |
| 1.2 | 32.577 | 20.788 | 21.592 | 19.827 | 18.732 | 23.428 | 33.097 | 34.710 | 50.850 |
| 1.3 | 35.292 | 22.521 | 23.391 | 21.480 | 20.292 | 25.381 | 35.855 | 37.603 | 55.087 |
| 1.4 | 38.007 | 24.253 | 25.190 | 23.132 | 21.853 | 27.333 | 38.613 | 40.496 | 59.325 |
| 1.5 | 40.722 | 25.985 | 26.990 | 24.784 | 23.414 | 29.286 | 41.371 | 43.388 | 63.562 |
| 1.6 | 43.437 | 27.718 | 28.789 | 26.437 | 24.975 | 31.238 | 44.129 | 46.281 | 67.800 |
| 1.7 | 46.151 | 29.450 | 30.588 | 28.089 | 26.536 | 33.190 | 46.887 | 49.173 | 72.037 |
| 1.8 | 48.866 | 31.182 | 32.388 | 29.741 | 28.097 | 35.143 | 49.645 | 52.066 | 76.275 |
| 1.9 | 51.581 | 32.915 | 34.187 | 31.394 | 29.658 | 37.095 | 52.403 | 54.958 | 80.512 |
| 2.0 | 54.296 | 34.647 | 35.986 | 33.046 | 31.219 | 39.047 | 55.161 | 57.851 | 84.750 |
| 2.1 | 57.011 | 36.379 | 37.786 | 34.698 | 32.780 | 41.000 | 57.920 | 60.743 | 88.987 |
| 2.2 | 59.725 | 38.112 | 39.585 | 36.350 | 34.341 | 42.952 | 60.678 | 63.636 | 93.225 |
| 2.3 | 62.440 | 39.844 | 41.384 | 38.003 | 35.902 | 44.905 | 63.436 | 66.528 | 97.462 |
| 2.4 | 65.155 | 41.576 | 43.184 | 39.655 | 37.463 | 46.857 | 66.194 | 69.421 | 101.700 |
| 2.5 | 67.870 | 43.309 | 44.983 | 41.307 | 39.024 | 48.809 | 68.952 | 72.313 | 105.937 |
| 2.6 | 70.585 | 45.041 | 46.782 | 42.960 | 40.585 | 50.762 | 71.710 | 75.206 | 110.175 |
| 2.7 | 73.299 | 46.773 | 48.581 | 44.612 | 42.146 | 52.714 | 74.468 | 78.099 | 114.412 |
| 2.8 | 76.014 | 48.506 | 50.381 | 46.264 | 43.707 | 54.666 | 77.226 | 80.991 | 118.650 |
| 2.9 | 78.729 | 50.238 | 52.180 | 47.916 | 45.268 | 56.619 | 79.984 | 83.884 | 122.887 |
| 3.0 | 81.444 | 51.971 | 53.979 | 49.569 | 46.829 | 58.571 | 82.742 | 86.776 | 127.125 |
| 3.1 | 84.159 | 53.703 | 55.779 | 51.221 | 48.390 | 60.524 | 85.500 | 89.539 | 131.366 |
| 3.2 | 86.873 | 55.435 | 57.578 | 52.873 | 49.951 | 62.476 | 88.258 | 94.701 | 135.640 |
| 3.3 | 89.588 | 57.168 | 59.377 | 54.526 | 51.512 | 64.428 | 91.016 | 100.877 | 139.573 |
| 3.4 | 92.303 | 58.900 | 61.177 | 56.178 | 53.073 | 66.381 | 93.775 | 107.274 | 143.098 |
| 3.5 | 95.018 | 60.632 | 62.976 | 57.830 | 54.634 | 68.333 | 96.533 | 113.342 | 146.209 |
| 3.6 | 97.732 | 62.365 | 64.775 | 59.482 | 56.195 | 70.285 | 99.291 | 118.500 | 148.983 |
| 3.7 | 100.447 | 64.097 | 66.575 | 61.135 | 57.756 | 72.238 | 102.049 | 122.848 | 151.436 |
| 3.8 | 103.162 | 65.829 | 68.374 | 62.787 | 59.317 | 74.190 | 104.807 | 126.252 | 153.565 |
| 3.9 | 105.877 | 67.562 | 70.173 | 64.439 | 60.877 | 76.142 | 107.565 | 129.585 | 155.300 |
| 4.0 | 108.592 | 69.294 | 71.973 | 66.092 | 62.438 | 78.095 | 110.323 | 133.078 | 156.694 |
| 4.1 | 111.306 | 71.026 | 73.772 | 67.744 | 63.999 | 80.047 | 113.081 | 135.914 | 157.918 |
| 4.2 | 114.021 | 72.759 | 75.571 | 69.396 | 65.560 | 82.000 | 115.839 | 139.253 | 158.697 |

| | | | | | | | | | |
|---|---|---|---|---|---|---|---|---|---|
| 4.3 | 116.736 | 74.491 | 77.371 | 71.048 | 66.996 | 83.952 | 118.522 | 141.961 | 159.444 |
| 4.4 | 119.451 | 76.223 | 79.170 | 72.701 | 68.255 | 85.904 | 123.141 | 144.742 | 159.784 |
| 4.5 | 122.166 | 77.956 | 80.969 | 74.353 | 69.446 | 87.857 | 128.204 | 147.661 | 160.201 |
| 4.6 | 124.880 | 79.688 | 82.768 | 76.005 | 70.607 | 89.809 | 133.587 | 150.415 | 160.315 |
| 4.7 | 127.595 | 81.421 | 84.568 | 77.658 | 71.774 | 91.761 | 139.145 | 153.129 | 160.481 |
| 4.8 | 130.310 | 83.251 | 86.065 | 79.318 | 72.955 | 93.714 | 144.959 | 155.798 | 160.625 |
| 4.9 | 133.025 | 85.296 | 86.907 | 80.995 | 74.167 | 95.666 | 151.066 | 158.407 | 160.980 |
| 5.0 | 135.740 | 87.314 | 87.493 | 82.599 | 75.408 | 117.923 | 155.892 | 3050.864 | 165.347 |

## Table 15 - Node Accelerations: Loma Prieta at Anderson Dam, $\xi$ =0.05

| | Link | | | | | | | | |
|---|---|---|---|---|---|---|---|---|---|
| Earthquake Intensity (g) | 1 | 2 | 3 | 4 | 5 | 6 | 7 | 8 | 9 |
| 0.1 | 3.220 | 1.471 | 1.811 | 1.857 | 1.659 | 1.740 | 2.088 | 2.576 | 3.508 |
| 0.2 | 6.440 | 2.943 | 3.623 | 3.714 | 3.318 | 3.480 | 4.176 | 5.152 | 7.017 |
| 0.3 | 9.660 | 4.414 | 5.434 | 5.571 | 4.977 | 5.220 | 6.263 | 7.728 | 10.526 |
| 0.4 | 12.880 | 5.885 | 7.246 | 7.428 | 6.636 | 6.961 | 8.351 | 10.304 | 14.034 |
| 0.5 | 16.100 | 7.356 | 9.057 | 9.285 | 8.295 | 8.701 | 10.439 | 12.880 | 17.543 |
| 0.6 | 19.320 | 8.828 | 10.869 | 11.142 | 9.954 | 10.441 | 12.527 | 15.455 | 21.051 |
| 0.7 | 22.540 | 10.299 | 12.680 | 12.999 | 11.613 | 12.181 | 14.615 | 18.031 | 24.560 |
| 0.8 | 25.760 | 11.770 | 14.492 | 14.856 | 13.272 | 13.921 | 16.703 | 20.607 | 28.068 |
| 0.9 | 28.980 | 13.242 | 16.303 | 16.712 | 14.931 | 15.661 | 18.790 | 23.183 | 31.577 |
| 1.0 | 32.200 | 14.713 | 18.115 | 18.570 | 16.590 | 17.401 | 20.878 | 25.759 | 35.085 |

## Table 16 - Node Accelerations: Loma Prieta at Coyote Lake Dam, $\xi$ =0.05

| | Link | | | | | | | | |
|---|---|---|---|---|---|---|---|---|---|
| Earthquake Intensity (g) | 1 | 2 | 3 | 4 | 5 | 6 | 7 | 8 | 9 |
| 0.1 | 3.149 | 2.419 | 3.171 | 3.593 | 3.750 | 3.568 | 3.339 | 5.100 | 6.315 |
| 0.2 | 6.298 | 4.839 | 6.341 | 7.186 | 7.501 | 7.137 | 6.678 | 10.200 | 12.631 |
| 0.3 | 9.447 | 7.258 | 9.512 | 10.778 | 11.251 | 10.705 | 10.018 | 15.300 | 18.946 |
| 0.4 | 12.596 | 9.677 | 12.683 | 14.371 | 15.002 | 14.273 | 13.357 | 20.400 | 25.261 |
| 0.5 | 15.745 | 12.096 | 15.853 | 17.964 | 18.752 | 17.841 | 16.696 | 25.500 | 31.576 |
| 0.6 | 18.894 | 14.516 | 19.024 | 21.556 | 22.502 | 21.410 | 20.035 | 30.599 | 37.891 |
| 0.7 | 22.043 | 16.935 | 22.194 | 25.149 | 26.253 | 24.978 | 23.374 | 35.699 | 44.207 |
| 0.8 | 25.192 | 19.354 | 25.365 | 28.742 | 30.003 | 28.546 | 26.714 | 40.799 | 50.522 |
| 0.9 | 28.341 | 21.774 | 28.536 | 32.335 | 33.753 | 32.115 | 30.053 | 45.899 | 56.837 |
| 1.0 | 31.490 | 24.193 | 31.706 | 35.927 | 37.504 | 35.683 | 33.392 | 50.999 | 63.152 |

## Table 17 - Node Accelerations: San Fernando at Hollywood, $\xi$ =0.03

| | Node | | | | | | | | |
|---|---|---|---|---|---|---|---|---|---|
| Earthquake Intensity (g) | 1 | 2 | 3 | 4 | 5 | 6 | 7 | 8 | 9 |
| 0.1 | 2.715 | 2.220 | 2.265 | 2.032 | 1.880 | 2.564 | 3.593 | 3.428 | 4.232 |
| 0.2 | 5.430 | 4.439 | 4.531 | 4.064 | 3.759 | 5.128 | 7.187 | 6.856 | 8.464 |
| 0.3 | 8.144 | 6.659 | 6.796 | 6.096 | 5.639 | 7.692 | 10.781 | 10.284 | 12.695 |
| 0.4 | 10.859 | 8.878 | 9.061 | 8.128 | 7.518 | 10.257 | 14.374 | 13.712 | 16.927 |
| 0.5 | 13.574 | 11.098 | 11.327 | 10.160 | 9.398 | 12.821 | 17.968 | 17.140 | 21.159 |
| 0.6 | 16.289 | 13.318 | 13.592 | 12.192 | 11.278 | 15.385 | 21.561 | 20.567 | 25.390 |
| 0.7 | 19.004 | 15.537 | 15.857 | 14.225 | 13.157 | 17.949 | 25.155 | 23.996 | 29.622 |
| 0.8 | 21.718 | 17.757 | 18.122 | 16.257 | 15.037 | 20.513 | 28.749 | 27.423 | 33.854 |
| 0.9 | 24.433 | 19.976 | 20.388 | 18.289 | 16.916 | 23.077 | 32.342 | 30.851 | 38.086 |
| 1.0 | 27.148 | 22.196 | 22.653 | 20.321 | 18.796 | 25.641 | 35.936 | 34.279 | 42.317 |
| 1.1 | 29.863 | 24.416 | 24.918 | 22.353 | 20.676 | 28.205 | 39.529 | 37.707 | 46.549 |
| 1.2 | 32.577 | 26.635 | 27.184 | 24.385 | 22.555 | 30.770 | 43.123 | 41.135 | 50.781 |
| 1.3 | 35.292 | 28.855 | 29.449 | 26.417 | 24.435 | 33.334 | 46.717 | 44.563 | 55.012 |
| 1.4 | 38.007 | 31.074 | 31.714 | 28.449 | 26.314 | 35.898 | 50.310 | 47.991 | 59.244 |
| 1.5 | 40.722 | 33.294 | 33.980 | 30.481 | 28.194 | 38.462 | 53.904 | 51.419 | 63.476 |
| 1.6 | 43.437 | 35.514 | 36.245 | 32.513 | 30.074 | 41.026 | 57.497 | 54.847 | 67.708 |
| 1.7 | 46.151 | 37.733 | 38.510 | 34.545 | 31.953 | 43.590 | 61.091 | 58.275 | 71.939 |
| 1.8 | 48.866 | 39.953 | 40.775 | 36.577 | 33.833 | 46.154 | 64.685 | 61.703 | 76.171 |
| 1.9 | 51.581 | 42.172 | 43.041 | 38.609 | 35.712 | 48.719 | 68.278 | 65.131 | 80.403 |
| 2.0 | 54.296 | 44.392 | 45.306 | 40.641 | 37.592 | 51.283 | 71.872 | 68.559 | 84.635 |
| 2.1 | 57.011 | 46.612 | 47.571 | 42.674 | 39.472 | 53.847 | 75.465 | 71.986 | 88.866 |
| 2.2 | 59.725 | 48.831 | 49.837 | 44.706 | 41.351 | 56.411 | 79.059 | 75.414 | 93.098 |
| 2.3 | 62.440 | 51.051 | 52.102 | 46.738 | 43.231 | 58.975 | 82.652 | 78.842 | 97.330 |
| 2.4 | 65.155 | 53.270 | 54.367 | 48.770 | 45.110 | 61.539 | 86.246 | 82.270 | 101.561 |
| 2.5 | 67.870 | 55.490 | 56.633 | 50.802 | 46.990 | 64.103 | 89.840 | 85.698 | 105.793 |
| 2.6 | 70.585 | 57.710 | 58.898 | 52.834 | 48.869 | 66.667 | 93.433 | 89.126 | 110.025 |
| 2.7 | 73.299 | 59.929 | 61.163 | 54.866 | 50.749 | 69.232 | 97.027 | 92.554 | 114.257 |
| 2.8 | 76.014 | 62.149 | 63.428 | 56.898 | 52.629 | 71.796 | 100.620 | 95.982 | 118.488 |
| 2.9 | 78.729 | 64.368 | 65.694 | 58.930 | 54.508 | 74.360 | 104.214 | 99.410 | 122.720 |
| 3.0 | 81.444 | 66.588 | 67.959 | 60.962 | 56.388 | 76.924 | 107.808 | 102.838 | 126.952 |
| 3.1 | 84.159 | 68.808 | 70.224 | 62.994 | 58.267 | 79.488 | 111.401 | 106.266 | 131.184 |
| 3.2 | 86.873 | 71.027 | 72.490 | 65.026 | 60.147 | 82.052 | 114.995 | 109.475 | 135.520 |
| 3.3 | 89.588 | 73.247 | 74.755 | 67.058 | 62.027 | 84.616 | 118.588 | 109.413 | 139.963 |
| 3.4 | 92.303 | 75.466 | 77.020 | 69.090 | 63.906 | 87.181 | 122.182 | 115.172 | 144.210 |
| 3.5 | 95.018 | 77.686 | 79.286 | 71.123 | 65.786 | 89.745 | 125.775 | 121.063 | 148.116 |
| 3.6 | 97.732 | 79.906 | 81.551 | 73.155 | 67.665 | 92.309 | 129.369 | 126.207 | 151.594 |
| 3.7 | 100.447 | 82.125 | 83.816 | 75.187 | 69.545 | 94.873 | 132.963 | 130.664 | 154.623 |
| 3.8 | 103.162 | 84.345 | 86.081 | 77.219 | 71.425 | 97.437 | 136.556 | 135.164 | 157.167 |
| 3.9 | 105.877 | 86.564 | 88.347 | 79.251 | 73.304 | 100.001 | 140.150 | 139.612 | 159.217 |
| 4.0 | 108.592 | 88.784 | 90.612 | 81.283 | 75.108 | 102.565 | 143.634 | 144.082 | 160.868 |

### Table 18 - Node Accelerations: Loma Prieta at Anderson Dam, $\xi$ =0.03

| Earthquake Intensity (g) | Node 1 | 2 | 3 | 4 | 5 | 6 | 7 | 8 | 9 |
|---|---|---|---|---|---|---|---|---|---|
| 0.1 | 3.220 | 1.808 | 2.272 | 2.192 | 1.908 | 2.438 | 2.699 | 2.641 | 3.657 |
| 0.2 | 6.440 | 3.616 | 4.545 | 4.383 | 3.816 | 4.876 | 5.398 | 5.282 | 7.315 |
| 0.3 | 9.660 | 5.424 | 6.817 | 6.575 | 5.724 | 7.313 | 8.097 | 7.923 | 10.972 |
| 0.4 | 12.880 | 7.232 | 9.089 | 8.767 | 7.632 | 9.751 | 10.796 | 10.564 | 14.630 |
| 0.5 | 16.100 | 9.040 | 11.362 | 10.958 | 9.540 | 12.189 | 13.495 | 13.205 | 18.287 |
| 0.6 | 19.320 | 10.848 | 13.634 | 13.150 | 11.448 | 14.626 | 16.194 | 15.846 | 21.945 |
| 0.7 | 22.540 | 12.657 | 15.907 | 15.342 | 13.357 | 17.064 | 18.893 | 18.488 | 25.602 |
| 0.8 | 25.760 | 14.465 | 18.179 | 17.533 | 15.265 | 19.502 | 21.591 | 21.129 | 29.260 |
| 0.9 | 28.980 | 16.273 | 20.451 | 19.725 | 17.173 | 21.940 | 24.290 | 23.770 | 32.917 |
| 1.0 | 32.200 | 18.081 | 22.724 | 21.917 | 19.081 | 24.377 | 26.989 | 26.411 | 36.575 |

### Table 19 - Node Accelerations: Loma Prieta at Coyote Lake Dam, $\xi$ =0.03

| Earthquake Intensity (g) | Node 1 | 2 | 3 | 4 | 5 | 6 | 7 | 8 | 9 |
|---|---|---|---|---|---|---|---|---|---|
| 0.1 | 3.149 | 3.133 | 4.055 | 4.655 | 4.76 | 4.702 | 4.311 | 6.671 | 8.7 |
| 0.2 | 6.298 | 6.266 | 8.11 | 9.311 | 9.519 | 9.405 | 8.623 | 13.343 | 17.401 |
| 0.3 | 9.447 | 9.399 | 12.165 | 13.967 | 14.279 | 14.107 | 12.934 | 20.015 | 26.101 |
| 0.4 | 12.596 | 12.532 | 16.22 | 18.623 | 19.039 | 18.81 | 17.246 | 26.687 | 34.802 |
| 0.5 | 15.745 | 15.666 | 20.275 | 23.278 | 23.798 | 23.512 | 21.558 | 33.358 | 43.502 |
| 0.6 | 18.894 | 18.799 | 24.33 | 27.934 | 28.558 | 28.214 | 25.869 | 40.03 | 52.202 |
| 0.7 | 22.043 | 21.932 | 28.385 | 32.589 | 33.318 | 32.917 | 30.181 | 46.702 | 60.903 |
| 0.8 | 25.192 | 25.065 | 32.44 | 37.245 | 38.077 | 37.619 | 34.492 | 53.373 | 69.603 |
| 0.9 | 28.341 | 28.198 | 36.496 | 41.901 | 42.837 | 42.322 | 38.804 | 60.045 | 78.304 |
| 1.0 | 31.49 | 31.331 | 40.55 | 46.556 | 47.597 | 47.024 | 43.115 | 66.717 | 87.004 |

## Table 20 - Node Accelerations: San Fernando at Hollywood, $\xi$ =0.01

| Earthquake Intensity (g) | Link 1 | 2 | 3 | 4 | 5 | 6 | 7 | 8 | 9 |
|---|---|---|---|---|---|---|---|---|---|
| 0.1 | 2.715 | 3.214 | 3.269 | 2.869 | 2.508 | 3.620 | 5.321 | 4.639 | 6.356 |
| 0.2 | 5.430 | 6.428 | 6.537 | 5.738 | 5.017 | 7.240 | 10.643 | 9.279 | 12.713 |
| 0.3 | 8.144 | 9.641 | 9.806 | 8.608 | 7.526 | 10.860 | 15.964 | 13.918 | 19.069 |
| 0.4 | 10.859 | 12.855 | 13.075 | 11.477 | 10.034 | 14.480 | 21.285 | 18.558 | 25.425 |
| 0.5 | 13.574 | 16.069 | 16.343 | 14.346 | 12.543 | 18.099 | 26.606 | 23.197 | 31.781 |
| 0.6 | 16.289 | 19.282 | 19.612 | 17.215 | 15.051 | 21.719 | 31.927 | 27.836 | 38.137 |
| 0.7 | 19.004 | 22.496 | 22.880 | 20.084 | 17.560 | 25.339 | 37.249 | 32.476 | 44.494 |
| 0.8 | 21.718 | 25.710 | 26.149 | 22.953 | 20.068 | 28.959 | 42.570 | 37.115 | 50.850 |
| 0.9 | 24.433 | 28.924 | 29.418 | 25.823 | 22.577 | 32.579 | 47.891 | 41.754 | 57.206 |
| 1.0 | 27.148 | 32.137 | 32.686 | 28.692 | 25.085 | 36.199 | 53.212 | 46.394 | 63.562 |
| 1.1 | 29.863 | 35.351 | 35.955 | 31.561 | 27.594 | 39.819 | 58.533 | 51.033 | 69.919 |
| 1.2 | 32.577 | 38.565 | 39.223 | 34.430 | 30.103 | 43.438 | 63.855 | 55.672 | 76.275 |
| 1.3 | 35.292 | 41.779 | 42.492 | 37.299 | 32.611 | 47.058 | 69.176 | 60.312 | 82.631 |
| 1.4 | 38.007 | 44.992 | 45.761 | 40.169 | 35.120 | 50.678 | 74.497 | 64.951 | 88.987 |
| 1.5 | 40.722 | 48.206 | 49.029 | 43.038 | 37.628 | 54.298 | 79.818 | 69.590 | 95.343 |
| 1.6 | 43.437 | 51.420 | 52.298 | 45.907 | 40.137 | 57.918 | 85.140 | 74.230 | 101.700 |
| 1.7 | 46.151 | 54.634 | 55.567 | 48.776 | 42.645 | 61.538 | 90.461 | 78.869 | 108.056 |
| 1.8 | 48.866 | 57.847 | 58.835 | 51.645 | 45.154 | 65.158 | 95.782 | 83.509 | 114.412 |
| 1.9 | 51.581 | 61.061 | 62.104 | 54.514 | 47.662 | 68.777 | 101.103 | 88.148 | 120.768 |
| 2.0 | 54.296 | 64.275 | 65.372 | 57.384 | 50.171 | 72.397 | 106.425 | 92.787 | 127.125 |
| 2.1 | 57.011 | 67.489 | 68.641 | 60.253 | 52.68 | 76.017 | 111.746 | 97.427 | 133.481 |
| 2.2 | 59.725 | 70.702 | 71.91 | 63.122 | 55.188 | 79.637 | 117.067 | 102.066 | 139.837 |
| 2.3 | 62.44 | 73.916 | 75.178 | 65.991 | 57.697 | 83.257 | 122.388 | 106.705 | 146.193 |
| 2.4 | 65.155 | 77.13 | 78.447 | 68.86 | 60.205 | 86.877 | 127.709 | 111.345 | 152.55 |
| 2.5 | 67.87 | 80.344 | 81.716 | 71.729 | 62.714 | 90.497 | 133.031 | 115.984 | 158.906 |
| 2.6 | 70.585 | 83.557 | 84.984 | 74.599 | 65.222 | 94.116 | 138.352 | 120.623 | 165.262 |
| 2.7 | 73.299 | 86.771 | 88.253 | 77.468 | 67.731 | 97.736 | 143.673 | 125.263 | 171.618 |
| 2.8 | 76.014 | 89.985 | 91.521 | 80.337 | 70.239 | 101.356 | 148.994 | 129.902 | 177.975 |
| 2.9 | 78.729 | 91.442 | 94.79 | 83.206 | 72.748 | 105.524 | 154.316 | 131.745 | 182.185 |
| 3.0 | 81.444 | 91.884 | 98.059 | 86.075 | 75.256 | 110.222 | 159.637 | 131.167 | 185.143 |

### Table 21 - Node Accelerations: Loma Prieta at Anderson Dam, $\xi$ =0.01

| Earthquake Intensity (g) | Link 1 | 2 | 3 | 4 | 5 | 6 | 7 | 8 | 9 |
|---|---|---|---|---|---|---|---|---|---|
| 0.1 | 3.220 | 3.137 | 3.269 | 2.871 | 2.898 | 3.753 | 4.028 | 3.278 | 5.603 |
| 0.2 | 6.440 | 6.273 | 6.538 | 5.742 | 5.797 | 7.507 | 8.056 | 6.557 | 11.206 |
| 0.3 | 9.660 | 9.410 | 9.808 | 8.612 | 8.695 | 11.260 | 12.083 | 9.835 | 16.808 |
| 0.4 | 12.880 | 12.547 | 13.077 | 11.483 | 11.594 | 15.014 | 16.111 | 13.114 | 22.411 |
| 0.5 | 16.100 | 15.683 | 16.346 | 14.354 | 14.492 | 18.767 | 20.139 | 16.393 | 28.014 |
| 0.6 | 19.320 | 18.820 | 19.615 | 17.225 | 17.391 | 22.520 | 24.166 | 19.671 | 33.617 |
| 0.7 | 22.540 | 21.956 | 22.885 | 20.096 | 20.289 | 26.274 | 28.194 | 22.950 | 39.220 |
| 0.8 | 25.760 | 25.093 | 26.154 | 22.966 | 23.188 | 30.027 | 32.222 | 26.228 | 44.822 |
| 0.9 | 28.980 | 28.229 | 29.423 | 25.837 | 26.086 | 33.781 | 36.250 | 29.506 | 50.425 |
| 1.0 | 32.200 | 31.366 | 32.692 | 28.708 | 28.985 | 37.534 | 40.277 | 32.785 | 56.028 |

### Table 22 - Node Accelerations: Loma Prieta at Coyote Lake Dam, $\xi$ =0.01

| Earthquake Intensity (g) | Link 1 | 2 | 3 | 4 | 5 | 6 | 7 | 8 | 9 |
|---|---|---|---|---|---|---|---|---|---|
| 0.1 | 3.149 | 4.358 | 5.766 | 6.956 | 7.551 | 7.259 | 6.719 | 10.147 | 14.346 |
| 0.2 | 6.298 | 8.716 | 11.533 | 13.913 | 15.102 | 14.518 | 13.439 | 20.295 | 28.693 |
| 0.3 | 9.447 | 13.073 | 17.299 | 20.869 | 22.653 | 21.777 | 20.159 | 30.443 | 43.039 |
| 0.4 | 12.596 | 17.431 | 23.066 | 27.826 | 30.204 | 29.036 | 26.879 | 40.591 | 57.386 |
| 0.5 | 15.745 | 21.789 | 28.832 | 34.782 | 37.755 | 36.295 | 33.598 | 50.738 | 71.731 |
| 0.6 | 18.894 | 26.147 | 34.598 | 41.739 | 45.306 | 43.553 | 40.317 | 60.886 | 86.077 |
| 0.7 | 22.043 | 30.505 | 40.365 | 48.695 | 52.857 | 50.813 | 47.037 | 71.034 | 100.424 |
| 0.8 | 25.192 | 34.863 | 46.131 | 55.652 | 60.408 | 58.071 | 53.757 | 81.181 | 114.770 |
| 0.9 | 28.341 | 39.221 | 51.456 | 62.766 | 68.786 | 65.483 | 60.392 | 89.953 | 128.369 |
| 1.0 | 31.490 | 43.630 | 57.076 | 70.015 | 79.788 | 71.334 | 67.718 | 96.181 | 133.413 |

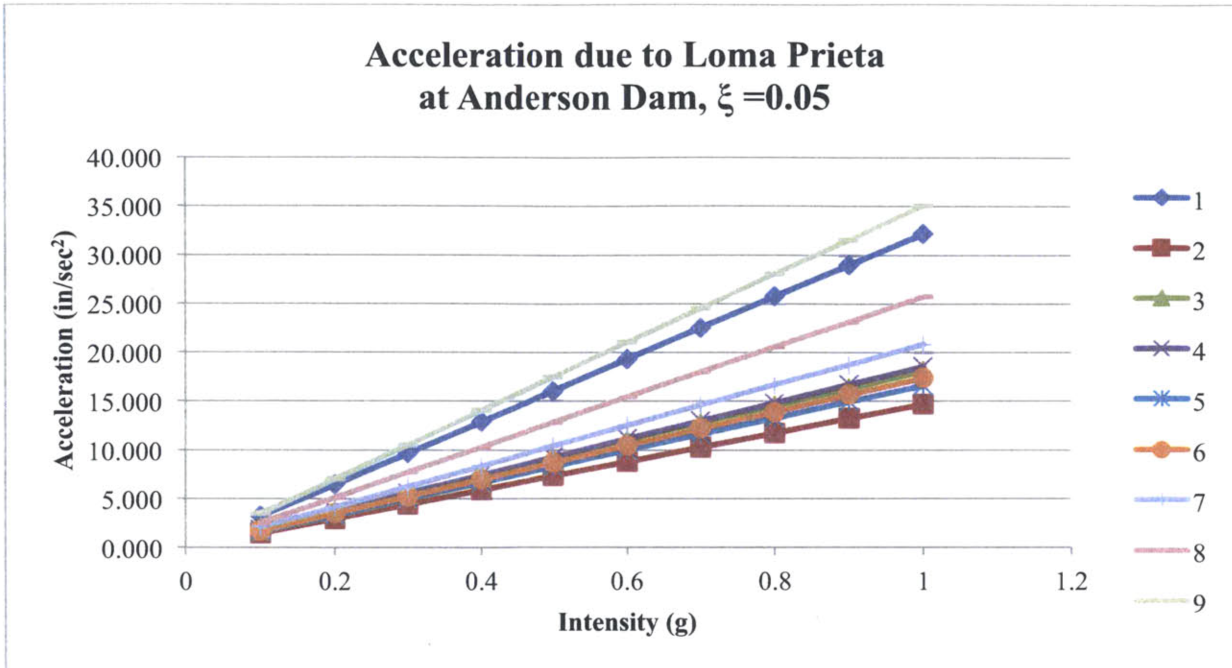


**Figure 35 - Nonlinear Accelerations for Loma Prieta at Anderson Dam, $\xi$ =0.05**

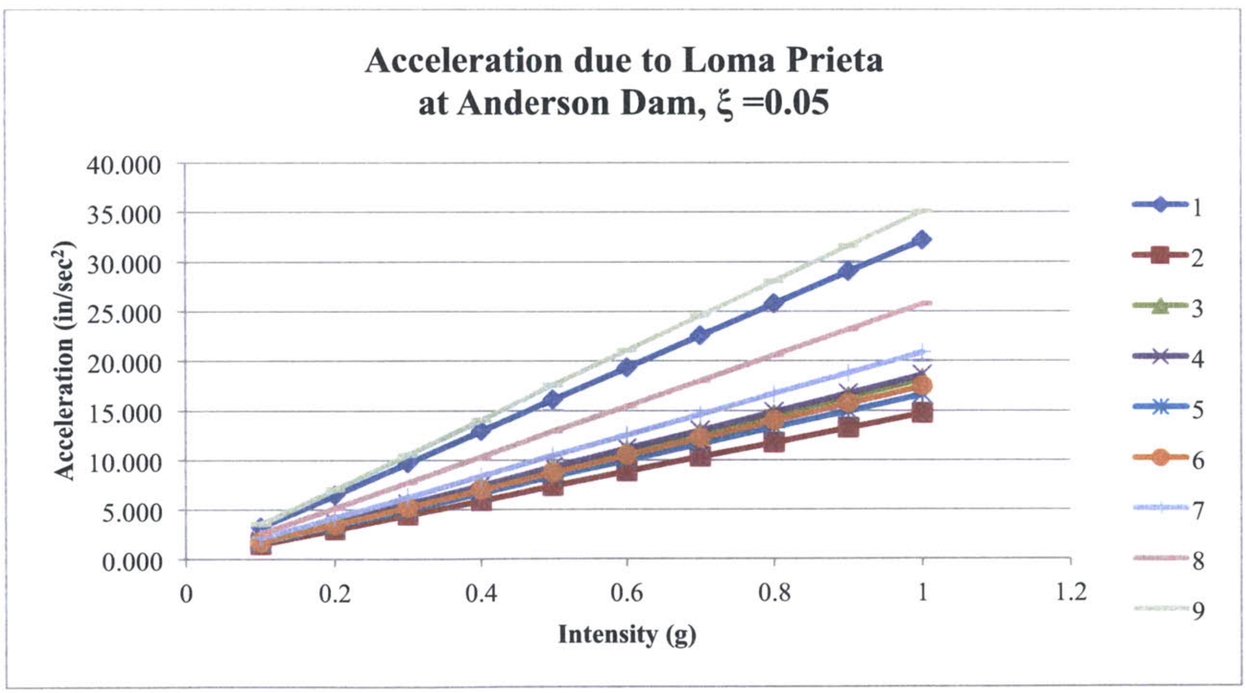


**Figure 36 - Linear Acceleration for Loma Prieta at Anderson Dam, $\xi$ =0.05**

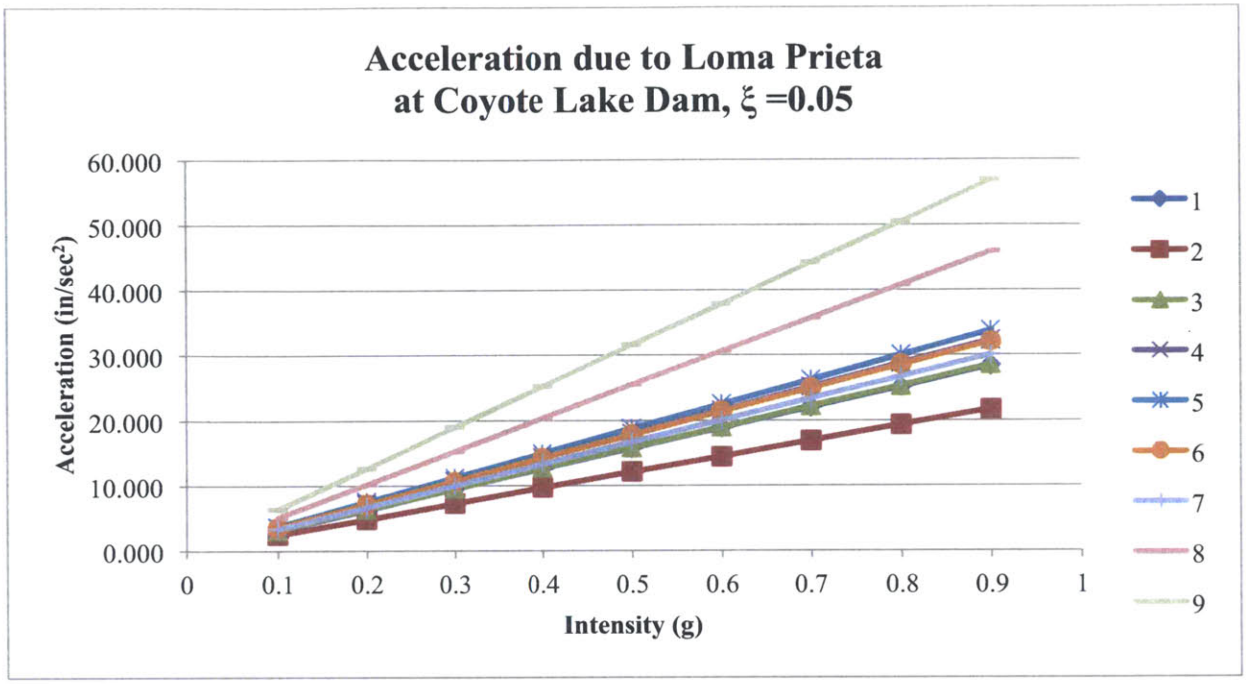


**Figure 37 - Nonlinear Accelerations for Loma Prieta at Coyote Lake Dam, $\xi$ =0.05**

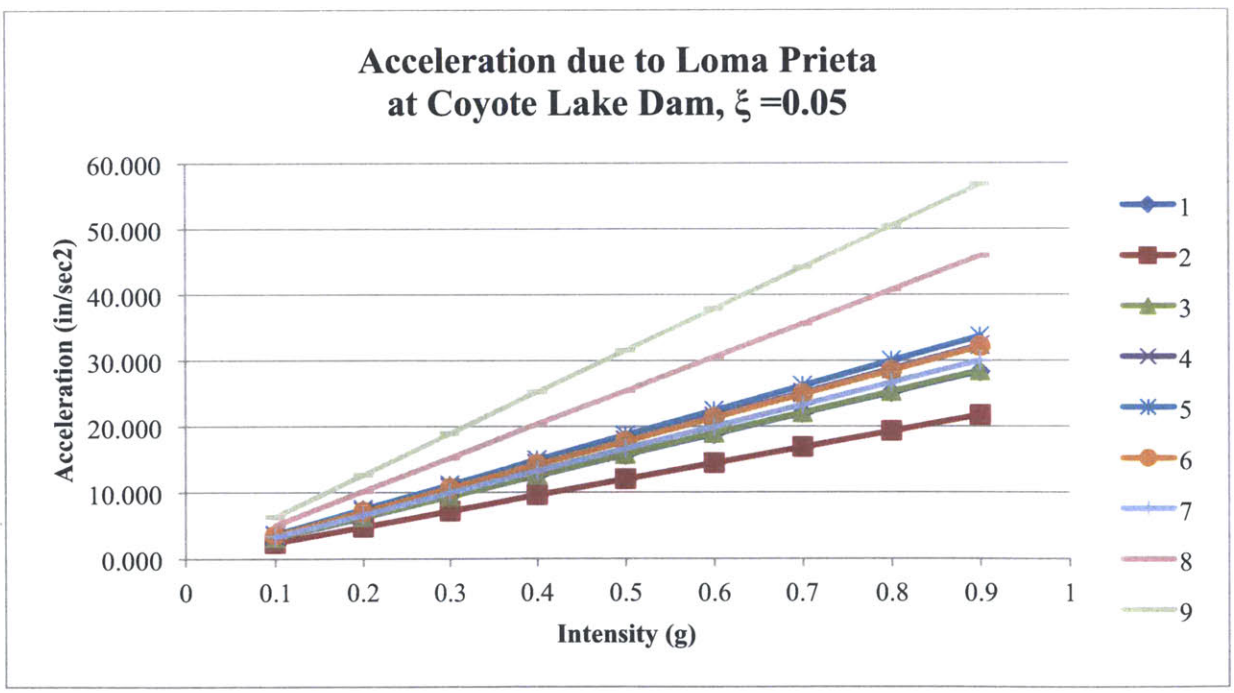


**Figure 38 - Linear Accelerations for Loma Prieta at Coyote Lake Dam, $\xi$ =0.05**

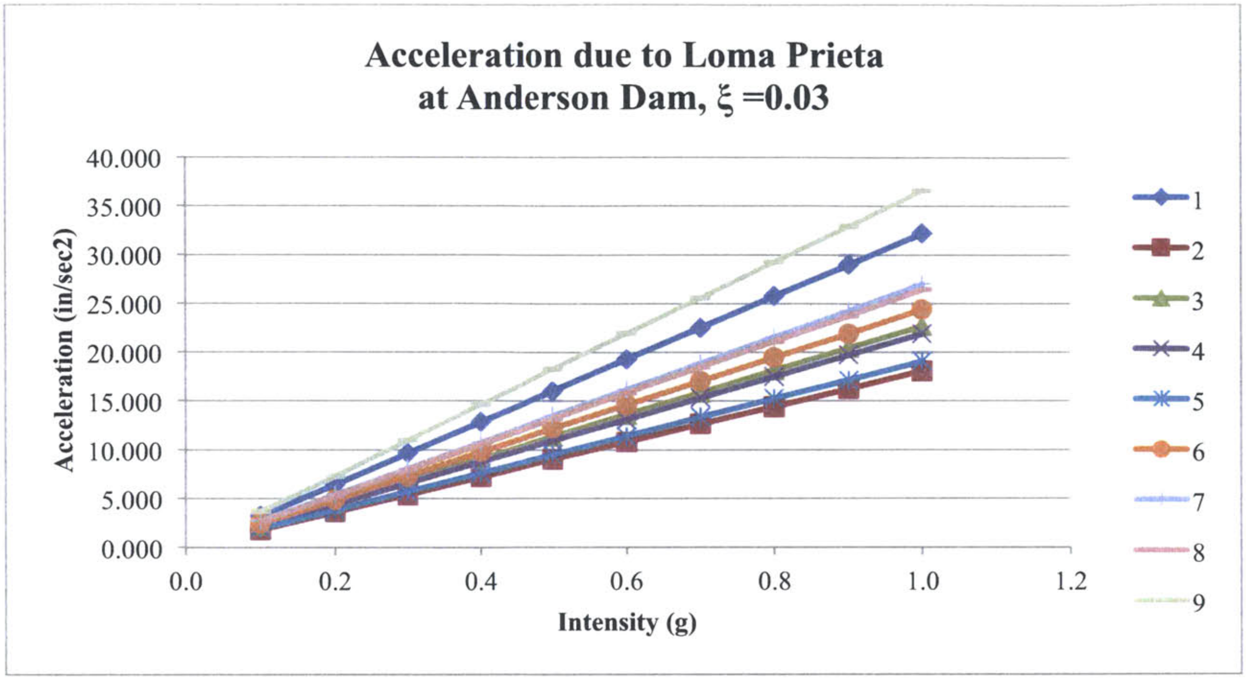


**Figure 39 - Nonlinear Accelerations for Loma Prieta at Anderson Dam, ξ =0.03**

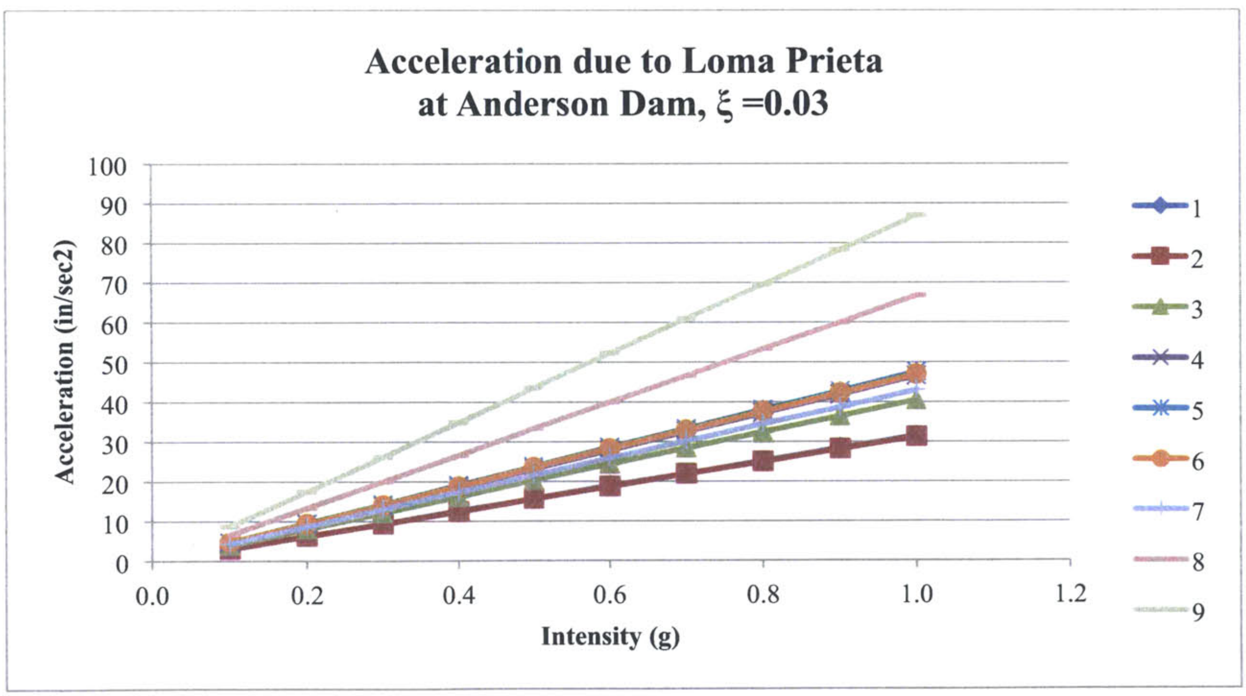


**Figure 40 - Nonlinear Accelerations for Loma Prieta at Coyote Lake Dam, ξ =0.03**

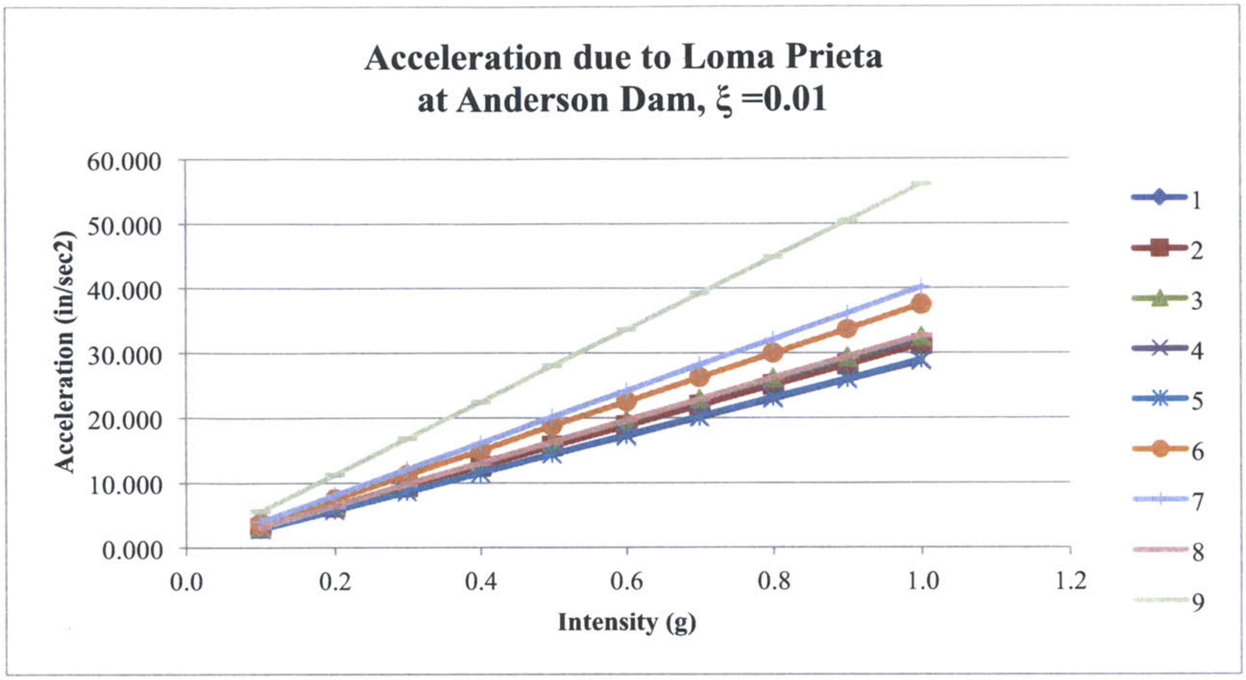


**Figure 41 - Nonlinear Accelerations for Loma Prieta at Anderson Dam, ξ =0.01**

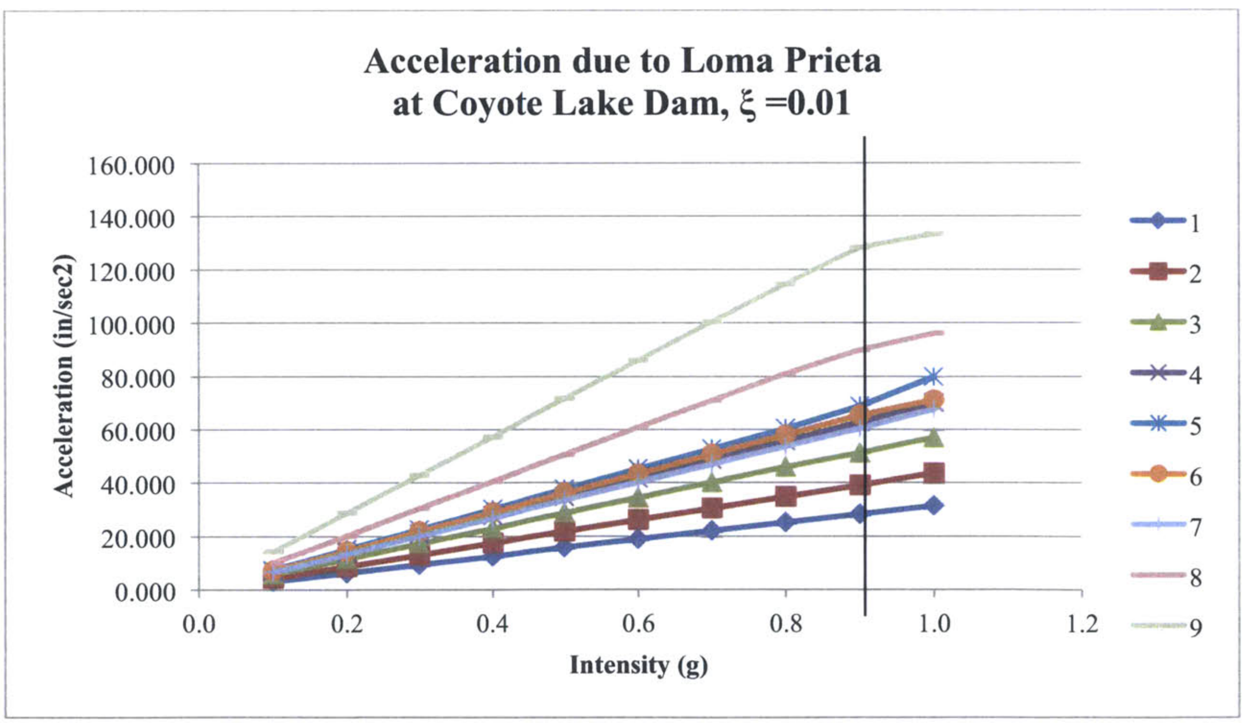


**Figure 42 - Nonlinear Accelerations for Loma Prieta at Coyote Lake Dam, ξ =0.01**